Layout: T1 Standard | Book ID: 330342_1_En | Book ISBN: 978-3-319-47796-1
Chapter No.: 6 | Date: 30-9-2016 Time: 7:37 pm | Page: 1/47

Improved Method for the Calculation of Plastic Rotation of Moment-Resisting Framed Structures for Nonlinear Static and Dynamic Analysis

Kevin K.F. Wong and Matthew S. Speicher

Abstract Given the vast advancements in computing power in the last several decades, nonlinear dynamic analysis has gained wide acceptance by practicing engineers as a useful way of assessing and improving the seismic performance of structures. Nonlinear structural analysis software packages give engineers the ability to directly model nonlinear component behavior in detail, resulting in improved understanding of how a building will respond under strong earthquake shaking. One key component, in particular, for understanding the behavior of moment-resisting frames is the plastic rotation of the flexural hinges. Performance-based standards typically use plastic rotation as the primary parameter for defining the acceptance criteria in moment-resisting frames. Since plastic rotation is a key parameter in the seismic damage assessment, the concept as well as the method to calculate this quantity must be understood completely. Though engineers rely on the plastic rotation output from seismic structural analysis software packages to determine acceptable performance, the actual calculation methods used in achieving such plastic rotation quantities usually lay within a so-called "black box". Based on the outputs obtained from most structural analysis software packages, it can be shown that running an algorithm considering material nonlinearity by itself will produce reasonably accurate results. Moreover, separately running an algorithm considering geometric nonlinearity also can produce accurate results. However, when material nonlinearity is combined with geometric nonlinearity in an analysis, obtaining accurate results or even stable solutions is more difficult. The coupling effect between the two nonlinearities can significantly affect the global response and the local plastic rotation obtained from the analysis and therefore needs to be verified through some analytical means. Yet, the verification process is difficult because a robust analytical framework for calculating plastic rotation is currently unavailable and urgently needed. In view of this gap, an analytical approach based on small displacement theory is derived using the force

K.K.F. Wong (✉) · M.S. Speicher
National Institute of Standards and Technology, Gaithersburg, MD 20899, USA
e-mail: kfwong@nist.gov

M.S. Speicher
e-mail: speicher@nist.gov

M. Papadrakakis et al. (eds.), *Computational Methods in Earthquake Engineering*,
Computational Methods in Applied Sciences 44,
DOI 10.1007/978-3-319-47798-5_6

Layout: T1 Standard | Book ID: 330342_1_En | Book ISBN: 978-3-319-47796-1
Chapter No.: 6 | Date: 30-9-2016 Time: 7:37 pm | Page: 2/47

analogy method to calculate the plastic rotations of plastic hinges at various locations of moment-resisting frames. Both static and dynamic analysis with nonlinear geometric effects will be incorporated in the derivation. Here the element stiffness matrices are first rigorously derived using a member with plastic hinges in compression, and therefore the coupling of geometric and material nonlinearity effects is included from the beginning of the derivation. Additionally, plastic rotation is handled explicitly by considering this rotation as an additional nonlinear degree-of-freedom. Numerical simulation is performed to calculate the nonlinear static and dynamic responses of simple benchmark models subjected to seismic excitations. Results are compared with various software packages to demonstrate the feasibility of the proposed method in light of the output results among software packages in calculating plastic rotations.

1 Introduction

Plastic rotation is one of the most fundamental structural performance metrics for moment-resisting frames. Current performance-based standards such as ASCE/SEI 41 [1] use plastic rotation as the primary performance measure in the assessment of flexure components in moment-resisting frames for the life safety and collapse prevention performance levels. Relatively large lateral displacement is expected to occur due to the flexibility of moment-resisting frames. Therefore, structural analysis software packages should possess the capability of handling both material nonlinearity and geometric nonlinearity in order to provide the needed output used to gauge acceptable performance.

Geometric nonlinearity causes a reduction in stiffness due to the axial compressive force acting on the entire length in the member, while material nonlinearity causes a reduction in stiffness concentrated at the plastic hinges of the member. These two nonlinear phenomena interact with one another in moment-resisting frames, but this interaction may have not been captured in all of the structural analysis software packages and algorithms that are currently available today. Yet, there have been studies concerning moment-resisting frames that involve the use of geometric nonlinearity with material nonlinearity in dynamic analysis (e.g., [2–6]) where the interaction is not explicitly handled but rather is left up to the software packages used in the analysis.

When addressing material nonlinearity, the plastic rotation action is often handled through a plastic reduction matrix, which represents the change in stiffness due to inelastic system behavior. This reduction matrix is derived using principles from the theory of plasticity and assuming an appropriate yield surface. It is often combined with the geometric stiffness matrix to account for both material and geometric nonlinearities and the behavior can then be traced incrementally by solving simultaneous linear algebraic equations to arrive at a solution. In other words, many of these seismic analysis software packages use one algorithm for

Layout: T1 Standard | Book ID: 330342_1_En | Book ISBN: 978-3-319-47796-1
Chapter No.: 6 | Date: 30-9-2016 Time: 7:37 pm | Page: 3/47

performing material nonlinearity analysis and another algorithm for performing geometric nonlinearity analysis.

Handling material nonlinearity and geometrically nonlinearity independently is often viewed as the most efficient approach for performing the analysis. It can be shown that running an algorithm considering material nonlinearity by itself will produce reasonably accurate results using most structural analysis software packages. Moreover, separately running an algorithm considering geometric nonlinearity also can produce reasonably accurate results. However, when material nonlinearity is combined with geometric nonlinearity in an analysis, software packages often neglect the interactions between these nonlinearities, resulting in limited consistency, reduced accuracy, and solution instability. As a result, plastic rotation, as the end product of the analysis, can differ significantly based on the approach taken in the nonlinear algorithm.

One reason for this shortcoming in addressing the nonlinear interaction is because currently there is no analytical theory that can be used to capture this interaction exactly. Therefore, a numerical solution is often employed that assumes the nonlinear interaction is automatically taken into account when both material and geometric nonlinearities are captured independently and then combined. The results presented here propose a method to accurately calculate the plastic rotation while capturing the interaction of material nonlinearity and geometric nonlinearity using an analytical theory based on basic principles of structural mechanics. Element stiffness matrices are first derived using a column member with plastic hinges subjected to axial compression; therefore, both geometric nonlinearity and material nonlinearity along with their interactions are captured from the beginning of the formulation. The element stiffness matrices are then assembled in the global stiffness matrices to perform nonlinear static analysis, and the global stiffness matrices are used in the dynamic equilibrium equations to perform nonlinear dynamic analysis. Numerical simulations are then performed on a simple moment-resisting frame. Both global responses such as the displacement and local responses including plastic rotations are obtained and compared with those obtained from various structural analysis software packages.

2 Element Stiffness Formulations

The stability theory of using stability functions is used to derive the element stiffness matrices of framed members with plastic hinges at both ends in a two-dimensional frame analysis. This theory was first developed for elastic structures in the 1960s [7–9], but it found limited application because of its complexity in the closed-form solution as compared to those using either the $P-\Delta$ approach [10] or the geometric stiffness approach [11]. Even with the advance in computing technology, only one research publication was found in the recent literature on the analysis of framed structures using stability functions [12]. For structures with significant lateral deflection, large geometric nonlinearity is expected, and linear or

Layout: T1 Standard | Book ID: 330342_1_En | Book ISBN: 978-3-319-47796-1
Chapter No.: 6 | Date: 30-9-2016 | Time: 7:37 pm | Page: 4/47

second-order approximation of the geometric nonlinearity may not be able to capture the nonlinear behavior accurately. Therefore, stability functions are rigorously derived in this paper to include both geometric and material nonlinearities in the element stiffness formulations.

2.1 *Element Stiffness Matrix* $[\mathbf{k}_i]$

The element stiffness matrix $\mathbf{k}_i$ for bending relates the displacement at the two ends of the ith member [commonly labeled as degrees of freedom (DOFs)] with the forces applied at these DOFs. For moment-resisting frame members, these displacement quantities include the lateral displacement and rotations at the two ends. This gives 4 DOFs for the bending stiffness of each element in a two-dimensional plane analysis, and these DOFs are labeled as:

- Case 1—Lateral displacement at the '1' end or 'near' end,
- Case 2—Rotation at the '1' end or 'near' end,
- Case 3—Lateral displacement at the '2' end or 'far' end, and
- Case 4—Rotation at the '2' end or 'far' end.

To compute the element stiffness matrix $\mathbf{k}_i$, each of the 4 DOFs is displaced independently by one unit as shown in Fig. 1 while subjected to an axial compressive load P. Here, V_{1l}, M_{1l}, V_{2l}, and M_{2l} represent the required shears and moments at the two ends of the member to cause the deflection in the prescribed pattern, and $l = 1, \ldots, 4$ represents the four cases of unit displacement patterns of member deflection.

Using the classical Bernoulli-Euler beam theory on homogeneous and isotropic material where the moment is proportional to the curvature and plane sections are assumed to remain plane, the governing equilibrium equation describing the deflected shape of the member can be written as

$$(EIv'')'' + Pv'' = 0 \tag{1}$$

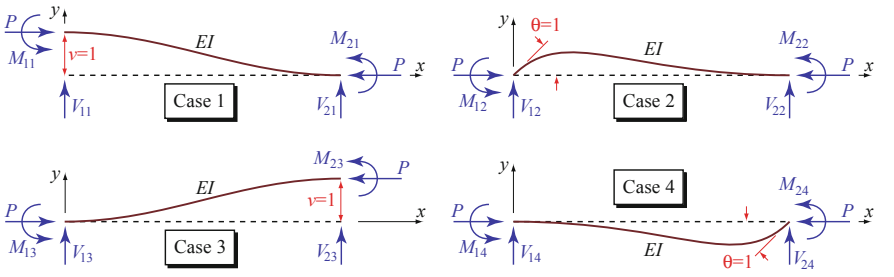

Fig. 1 Displacement patterns and the corresponding fixed-end forces

Layout: T1 Standard | Book ID: 330342_1_En | Book ISBN: 978-3-319-47796-1
Chapter No.: 6 | Date: 30-9-2016 Time: 7:37 pm | Page: 5/47

where E is the elastic modulus, I is the moment of inertia, v is the lateral deflection, P is the axial compressive force of the member, and each prime represents taking derivatives of the corresponding variable with respect to the x-direction of the member. By assuming EI is constant along the member, the solution to the fourth-order ordinary differential equation becomes:

$$v = A\ \sin kx + B\ \cos kx + Cx + D \tag{2}$$

where $k^2 = P/EI$. Let $\lambda = kL$ to simplify the derivations, where L is the length of the member. The following four cases of boundary conditions (in reverse order) are now considered.

Case 4 of Fig. 1: Imposing the boundary conditions $v(0) = 0$, $v'(0) = 0$, $v(L) = 0$, and $v'(L) = 1$ gives

$$v(0) = 0: \quad B + D = 0 \tag{3a}$$

$$v'(0) = 0: \quad kA + C = 0 \tag{3b}$$

$$v(L) = 0: \quad A\ \sin\lambda + B\ \cos\lambda + CL + D = 0 \tag{3c}$$

$$v'(L) = 1: \quad kA\ \cos\lambda - kB\ \sin\lambda + C = 1 \tag{3d}$$

Solving simultaneously for the constants in Eqs. 3a–3d gives

$$A = \frac{L(1-\cos\lambda)}{\lambda(\lambda\ \sin\lambda + 2\ \cos\lambda - 2)}, \quad B = \frac{L(\sin\lambda - \lambda)}{\lambda(\lambda\ \sin\lambda + 2\ \cos\lambda - 2)}, \quad C = -kA, \quad D = -B$$

Therefore, Eq. 2 along with the constants in Eq. 4 gives the deflected shape for Case 4. The shears (i.e., V_{14} and V_{24}) and moments (i.e., M_{14} and M_{24}) at the two ends of the member (see Fig. 1) are then evaluated using the classical Bernoulli-Euler beam theory formula:

$$M(x) = EIv'', \quad V(x) = EIv''' + Pv' \tag{5}$$

Now taking derivatives of Eq. 2 and substituting the results into Eq. 5 while using the constants calculated in Eq. 4, the shears and moments at the two ends for Case 4 in Fig. 1 are calculated as:

$$M_{14} = -EIv''(0) = EIk^2B = scEI/L \tag{6a}$$

$$V_{14} = EIv'''(0) + Pv'(0) = -EIk^3A + P \times 0 = \bar{s}EI/L^2 \tag{6b}$$

$$M_{24} = EIv''(L) = -EIk^2(A\ \sin\lambda + B\ \cos\lambda) = sEI/L \tag{6c}$$

Layout: T1 Standard | Book ID: 330342_1_En | Book ISBN: 978-3-319-47796-1
Chapter No.: 6 | Date: 30-9-2016 | Time: 7:37 pm | Page: 6/47

$$V_{24} = -EIv'''(L) - Pv'(L) = EIk^3(A\cos\lambda - B\sin\lambda) - P \times 1 = -\bar{s}EI/L^2 \quad (6d)$$

where

$$s = \frac{\lambda(\sin\lambda - \lambda\cos\lambda)}{2 - 2\cos\lambda - \lambda\sin\lambda}, \quad c = \frac{\lambda - \sin\lambda}{\sin\lambda - \lambda\cos\lambda}, \quad \bar{s} = s + sc = \frac{\lambda^2(1-\cos\lambda)}{2 - 2\cos\lambda - \lambda\sin\lambda} \quad (7)$$

The minus signs appear in front of the equations for M_{14} in Eq. 6a and V_{24} in Eq. 6d because there is a difference in sign convention between the classical Bernoulli-Euler beam theory and the theory for the stiffness method in structural analysis.

Case 3 of Fig. 1: Imposing the boundary conditions $v(0) = 0$, $v'(0) = 0$, $v(L) = 1$, and $v'(L) = 0$ gives

$$v(0) = 0: \quad B + D = 0 \quad (8a)$$

$$v'(0) = 0: \quad kA + C = 0 \quad (8b)$$

$$v(L) = 1: \quad A\sin\lambda + B\cos\lambda + CL + D = 1 \quad (8c)$$

$$v'(L) = 0: \quad kA\cos\lambda - kB\sin\lambda + C = 0 \quad (8d)$$

Solving simultaneously for the constants in Eqs. 8a–8d gives

$$A = -\frac{\sin\lambda}{\lambda\sin\lambda + 2\cos\lambda - 2}, \quad B = \frac{1-\cos\lambda}{\lambda\sin\lambda + 2\cos\lambda - 2}, \quad C = -kA, \quad D = -B \quad (9)$$

Therefore, Eq. 2 along with the constants in Eq. 9 gives the deflected shape for Case 3. Now taking derivatives of Eq. 2 and substituting the results into Eq. 5 while using the constants calculated in Eq. 9, the shears and moments at the two ends for Case 3 in Fig. 1 are calculated as:

$$M_{13} = -EIv''(0) = EIk^2B = -\bar{s}EI/L^2 \quad (10a)$$

$$V_{13} = EIv'''(0) + Pv'(0) = -EIk^3A + P \times 0 = -s'EI/L^3 \quad (10b)$$

$$M_{23} = EIv''(L) = -EIk^2(A\sin\lambda + B\cos\lambda) = -\bar{s}EI/L^2 \quad (10c)$$

$$V_{23} = -EIv'''(L) - Pv'(L) = EIk^3(A\cos\lambda - B\sin\lambda) - P \times 0 = s'EI/L^3 \quad (10d)$$

where

Layout: T1 Standard | Book ID: 330342_1_En | Book ISBN: 978-3-319-47796-1
Chapter No.: 6 | Date: 30-9-2016 Time: 7:37 pm | Page: 7/47

$$s' = 2\bar{s} - \lambda^2 = \frac{\lambda^3 \sin\lambda}{2 - 2\cos\lambda - \lambda\sin\lambda} \tag{11}$$

and $\bar{s}$ is given in Eq. 7.

Case 2 of Fig. 1: Imposing the boundary conditions $v(0) = 0$, $v'(0) = 1$, $v(L) = 0$, and $v'(L) = 0$ gives

$$v(0) = 0: \quad B + D = 0 \tag{12a}$$

$$v'(0) = 1: \quad kA + C = 1 \tag{12b}$$

$$v(L) = 0: \quad A\sin\lambda + B\cos\lambda + CL + D = 0 \tag{12c}$$

$$v'(L) = 0: \quad kA\cos\lambda - kB\sin\lambda + C = 0 \tag{12d}$$

Solving simultaneously for the constants in Eqs. 12a–12d gives

$$A = \frac{L(\lambda\sin\lambda + \cos\lambda - 1)}{\lambda(\lambda\sin\lambda + 2\cos\lambda - 2)}, \quad B = \frac{L(\lambda\cos\lambda - \sin\lambda)}{\lambda(\lambda\sin\lambda + 2\cos\lambda - 2)}, \quad C = 1 - kA, \quad D = -B \tag{13}$$

Therefore, Eq. 2 along with the constants in Eq. 13 gives the deflected shape for Case 2. Now taking derivatives of Eq. 2 and substituting the results into Eq. 5 while using the constants calculated in Eq. 13, the shears and moments at the two ends for Case 2 in Fig. 1 are calculated as:

$$M_{12} = -EIv''(0) = EIk^2B = sEI/L \tag{14a}$$

$$V_{12} = EIv'''(0) + Pv'(0) = -EIk^3A + P \times 1 = \bar{s}EI/L^2 \tag{14b}$$

$$M_{22} = EIv''(L) = -EIk^2(A\sin\lambda + B\cos\lambda) = scEI/L \tag{14c}$$

$$V_{22} = -EIv'''(L) - Pv'(L) = EIk^3(A\cos\lambda - B\sin\lambda) - P \times 0 = -\bar{s}EI/L^2 \tag{14d}$$

where s, c, and $\bar{s}$ are given in Eq. 7.

Case 1 of Fig. 1: Finally, imposing the boundary conditions $v(0) = 1$, $v'(0) = 0$, $v(L) = 0$, and $v'(L) = 0$ gives

$$v(0) = 1: \quad B + D = 1 \tag{15a}$$

$$v'(0) = 0: \quad kA + C = 0 \tag{15b}$$

Layout: T1 Standard | Book ID: 330342_1_En | Book ISBN: 978-3-319-47796-1
Chapter No.: 6 | Date: 30-9-2016 | Time: 7:37 pm | Page: 8/47

$$v(L) = 0: \quad A\ \sin\lambda + B\ \cos\lambda + CL + D = 0 \tag{15c}$$

$$v'(L) = 0: \quad kA\ \cos\lambda - kB\ \sin\lambda + C = 0 \tag{15d}$$

Solving simultaneously for the constants in Eqs. 15a–15d gives

$$A = \frac{\sin\lambda}{\lambda\ \sin\lambda + 2\ \cos\lambda - 2}, \quad B = \frac{\cos\lambda - 1}{\lambda\ \sin\lambda + 2\ \cos\lambda - 2}, \quad C = -kA, \quad D = 1 - B \tag{16}$$

Therefore, Eq. 2 along with the constants in Eq. 16 gives the deflected shape for Case 1. Now taking derivatives of Eq. 2 and substituting the results into Eq. 5 while using the constants calculated in Eq. 16, the shears and moments at the two ends for Case 1 in Fig. 1 are calculated as:

$$M_{11} = -EIv''(0) = EIk^2B = \bar{s}EI/L^2 \tag{17a}$$

$$V_{11} = EIv'''(0) + Pv'(0) = -EIk^3A + P \times 0 = s'EI/L^3 \tag{17b}$$

$$M_{21} = EIv''(L) = -EIk^2(A\ \sin\lambda + B\ \cos\lambda) = \bar{s}EI/L^2 \tag{17c}$$

$$V_{21} = -EIv'''(L) - Pv'(L) = EIk^3(A\ \cos\lambda - B\ \sin\lambda) - P \times 0 = -s'EI/L^3 \tag{17d}$$

where $\bar{s}$ is given in Eq. 7 and s' is given in Eq. 11.

In summary, based on Eqs. 6a–6d, 10a–10d, 14a–14d, and 17a–17d for the above four cases, the element stiffness matrix of the ith member $\mathbf{k}_i$ after incorporating axial compressive force using stability functions becomes:

$$\mathbf{k}_i = \frac{EI}{L^3}\begin{bmatrix} s' & \bar{s}L & -s' & \bar{s}L \\ \bar{s}L & sL^2 & -\bar{s}L & scL^2 \\ -s' & -\bar{s}L & s' & -\bar{s}L \\ \bar{s}L & scL^2 & -\bar{s}L & sL^2 \end{bmatrix} \begin{matrix} \leftarrow v(0) \\ \leftarrow v'(0) \\ \leftarrow v(L) \\ \leftarrow v'(L) \end{matrix} \tag{18}$$

2.2 *Element Stiffness Matrix* $[\mathbf{k}_i']$

The element stiffness matrix $\mathbf{k}_i'$ relates the plastic rotations at the plastic hinge locations (PHLs) of the ith member with the restoring forces applied at the DOFs. Two plastic hinges typically occur at the two ends of the member, and they are

Layout: T1 Standard | Book ID: 330342_1_En | Book ISBN: 978-3-319-47796-1
Chapter No.: 6 | Date: 30-9-2016 Time: 7:37 pm | Page: 9/47

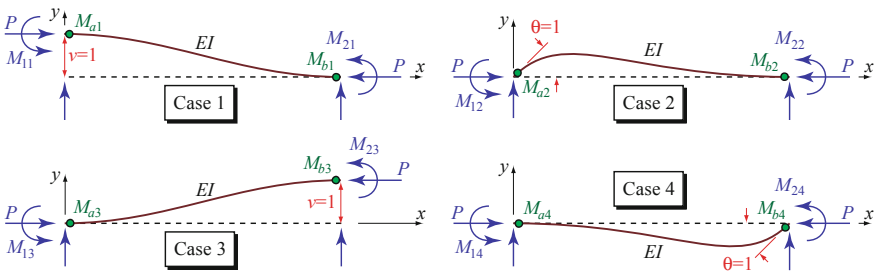

Fig. 2 Displacement patterns for computation of moments at the plastic hinge locations

labeled as 'a' for plastic hinge at the 'near' end (or '1' end) and 'b' for plastic hinge at the 'far' end (or '2' end) as shown in Fig. 2. To compute the element stiffness matrix $\mathbf{k}_i'$, a unit plastic rotation at each PHL is independently applied to the member and then determine the shear and moment at each of the two ends. However, this is a difficult process because imposing a unit plastic rotation requires the discontinuity of $v'(x)$ to be addressed. To avoid this problem, the $\mathbf{k}_i'^T$ matrix is constructed instead. The $\mathbf{k}_i'^T$ matrix relates the lateral displacements and rotations at the two ends of the member (i.e., the four cases of unit displacements at each DOF) with the moments at the PHLs (i.e., M_{al} and M_{bl}, $l = 1, \ldots, 4$).

Consider the four cases of unit displacements of the member independently as shown in Fig. 2, where the moment at the plastic hinges 'a' and 'b' (i.e., M_{al} and M_{bl}, $l = 1, \ldots, 4$) represent the desired quantities. Note that the moments at the two ends of the member (i.e., M_{1l} and M_{2l}, $l = 1, \ldots, 4$) have already been calculated using the unit displacement patterns in Fig. 1 and summarized in the second and fourth rows of the element stiffness matrix $\mathbf{k}_i$ given in Eq. 18. Therefore, based on Fig. 2, the moments M_{al} and M_{bl} at the two plastic hinges for each of the four cases become:

Case 1 of Fig. 2: Imposing the boundary conditions $v(0) = 1$, $v'(0) = 0$, $v(L) = 0$, and $v'(L) = 0$ gives

$$M_{a1} = M_{11} = \bar{s}EI/L^2, \quad M_{b1} = M_{21} = \bar{s}EI/L^2 \tag{19}$$

Case 2 of Fig. 2: Imposing the boundary conditions $v(0) = 0$, $v'(0) = 1$, $v(L) = 0$, and $v'(L) = 0$ gives

$$M_{a2} = M_{12} = sEI/L, \quad M_{b2} = M_{22} = scEI/L \tag{20}$$

Case 3 of Fig. 2: Imposing the boundary conditions $v(0) = 0$, $v'(0) = 0$, $v(L) = 1$, and $v'(L) = 0$ gives

$$M_{a3} = M_{13} = -\bar{s}EI/L^2, \quad M_{b3} = M_{23} = -\bar{s}EI/L^2 \tag{21}$$

Layout: T1 Standard | Book ID: 330342_1_En | Book ISBN: 978-3-319-47796-1
Chapter No.: 6 | Date: 30-9-2016 Time: 7:37 pm | Page: 10/47

Case 4 of Fig. 2: Finally, imposing the boundary conditions $v(0) = 0$, $v'(0) = 0$, $v(L) = 0$, and $v'(L) = 1$ gives

$$M_{a4} = M_{14} = scEI/L, \quad M_{b4} = M_{24} = sEI/L \tag{22}$$

Therefore, from Eqs. 19 to 22, the transpose of stiffness matrix $\mathbf{k}_i'$ for the ith member becomes

$$\mathbf{k}_i'^T = \begin{bmatrix} \bar{s}EI/L^2 & sEI/L & -\bar{s}EI/L^2 & scEI/L \\ \bar{s}EI/L^2 & scEI/L & -\bar{s}EI/L^2 & sEI/L \end{bmatrix} \begin{matrix} \leftarrow \theta_a'' \\ \leftarrow \theta_b'' \end{matrix} \tag{23}$$

Once the $\mathbf{k}_i'^T$ matrix in Eq. 23 is derived, the $\mathbf{k}_i'$ matrix can be written as:

$$\mathbf{k}_i' = \begin{bmatrix} M_{a1} & M_{b1} \\ M_{a2} & M_{b2} \\ M_{a3} & M_{b3} \\ M_{a4} & M_{b4} \end{bmatrix} = \begin{bmatrix} \bar{s}EI/L^2 & \bar{s}EI/L^2 \\ sEI/L & scEI/L \\ -\bar{s}EI/L^2 & -\bar{s}EI/L^2 \\ scEI/L & sEI/L \end{bmatrix} \begin{matrix} \leftarrow v(0) \\ \leftarrow v'(0) \\ \leftarrow v(L) \\ \leftarrow v'(L) \end{matrix} \tag{24}$$

2.3 *Element Stiffness Matrix* $[\mathbf{k}_i'']$

The element stiffness matrix $\mathbf{k}_i''$ relates the moments at the PHLs 'a' and 'b' with a corresponding unit plastic rotation at each of these PHLs of the ith member. To determine the $\mathbf{k}_i''$ matrix, the goal is to compute the plastic hinge moments M_{aa}, M_{ab}, M_{ba}, and M_{bb} as shown in Fig. 3.

The moments computed in the process of determining the 4×2 $\mathbf{k}_i'$ matrix shown in Eq. 24 can be used to calculate the element stiffness matrix $\mathbf{k}_i''$. For example, the first column of the $\mathbf{k}_i'$ matrix in Eq. 24 represents the shears ($V_{near} = M_{a1} = \bar{s}EI/L^2$ and $V_{far} = M_{a3} = -\bar{s}EI/L^2$) and moments ($M_{a2} = sEI/L$ and $M_{a4} = scEI/L$) at the two ends of the member due to a unit plastic rotation at PHL 'a', as shown in Fig. 3. Similarly, the second column of the $\mathbf{k}_i'$ matrix in Eq. 24 represents the shears ($V_{near} = M_{b1} = \bar{s}EI/L^2$ and $V_{far} = M_{b3} = -\bar{s}EI/L^2$) and moments ($M_{b2} = scEI/L$ and $M_{b4} = sEI/L$) at the two ends of the member due to a unit plastic rotation at PHL 'b', as shown in Fig. 3. Then the plastic hinge moments M_{aa}, M_{ab}, M_{ba}, and M_{bb} at the PHLs for each of the two cases (i.e., 'a' and 'b') can be evaluated as:

Case '*a*' of Fig. 3: Imposing a unit plastic rotation $\theta_a'' = 1$ and $\theta_b'' = 0$ gives

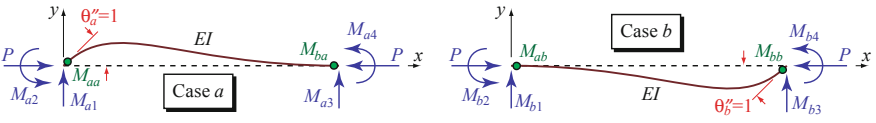

Fig. 3 Displacement patterns for computation of moments due to unit plastic rotations

Layout: T1 Standard | Book ID: 330342_1_En | Book ISBN: 978-3-319-47796-1
Chapter No.: 6 | Date: 30-9-2016 Time: 7:37 pm | Page: 11/47

$$M_{aa} = M_{a2} = sEI/L, \quad M_{ba} = M_{a4} = scEI/L \tag{25}$$

Case '*b*' of Fig. 3: Imposing a unit plastic rotation $\theta''_a = 0$ and $\theta''_b = 1$ gives

$$M_{ab} = M_{b2} = scEI/L, \quad M_{bb} = M_{b4} = sEI/L \tag{26}$$

Therefore, from Eqs. 25 and 26, the element stiffness matrix $\mathbf{k}''_i$ for the ith member becomes

$$\mathbf{k}''_i = \begin{bmatrix} sEI/L & scEI/L \\ scEI/L & sEI/L \end{bmatrix} \begin{matrix} \leftarrow \theta''_a \\ \leftarrow \theta''_b \end{matrix} \tag{27}$$

3 Global Stiffness Matrices

By using the element stiffness matrices computed in Eqs. 18, 24, and 27, the assembly of these matrices into the global stiffness matrices $\mathbf{K}$, $\mathbf{K}'$, and $\mathbf{K}''$ is a straightforward procedure; many textbooks (e.g., [11, 13, 14]) have discussed this procedure in great detail. The procedure is to map each DOFs and PHLs of the element stiffness matrices to the corresponding DOFs and PHLs of the global stiffness matrices. Consider a framed structure having a total of n DOFs and m PHLs, the resulting global stiffness matrices can then be obtained and are often written in the form:

$$\mathbf{K} = \Big[\, \textit{Collection of } \mathbf{k}_i \,\Big]_{n\times n} \begin{matrix} \leftarrow DOF\ \#1 \\ \vdots \\ \leftarrow DOF\ \#n \end{matrix} \tag{28a}$$

$$\mathbf{K}' = \Big[\, \textit{Collection of } \mathbf{k}'_i \,\Big]_{n\times m} \begin{matrix} \leftarrow DOF\ \#1 \\ \vdots \\ \leftarrow DOF\ \#n \end{matrix} \tag{28b}$$

$$\mathbf{K}'' = \Big[\, \textit{Collection of } \mathbf{K}''_i \,\Big]_{m\times m} \begin{matrix} \leftarrow PHL\ \#1 \\ \vdots \\ \leftarrow PHL\ \#m \end{matrix} \tag{28c}$$

However, consistencies of the global stiffness matrices depend on the consistencies of the element stiffness matrices, and therefore it is worth spending the effort to investigate the properties of the element stiffness matrix $\mathbf{k}_i$ computed in Eq. 18 and its relationship with the global stiffness matrix $\mathbf{K}$ in Eq. (28a).

The element stiffness matrix $\mathbf{k}_i$ is obtained by solving the fourth order differential equation, and therefore it is the exact solution based on small displacement theory. It is a nonlinear relationship with sine and cosine functions of the axial compressive force P, and it is capable of capturing both large $P{-}\Delta$ (i.e., geometric nonlinearity due to sidesway of the member) and small $P{-}\delta$ (i.e., geometric nonlinearity due to local deformation of the member) effects. One can perform Taylor series expansion of Eq. 18 with respect to P and then truncating the higher-order terms. Doing so gives

$$\mathbf{k}_{i(GS)} = \frac{EI}{L^3}\begin{bmatrix} 12 & 6L & -12 & 6L \\ 6L & 4L^2 & -6L & 2L^2 \\ -12 & -6L & 12 & -6L \\ 6L & 2L^2 & -6L & 4L^2 \end{bmatrix} + \frac{P}{L}\begin{bmatrix} -6/5 & -L/10 & 6/5 & -L/10 \\ -L/10 & -2L^2/15 & L/10 & L^2/30 \\ 6/5 & L/10 & -6/5 & L/10 \\ -L/10 & L^2/30 & L/10 & -2L^2/15 \end{bmatrix} \tag{29}$$

where $\mathbf{k}_{i(GS)}$ is commonly known as the second-order geometric stiffness of the member, with the first term representing the initial elastic stiffness matrix and the second term representing the geometric stiffness matrix. Since $\mathbf{k}_{i(GS)}$ is obtained by Taylor series expansion, both large $P{-}\Delta$ and small $P{-}\delta$ effects are also captured in this formulation.

Further simplification of Eq. 29 can be performed by ignoring the small $P{-}\delta$ effect, and the resulting element stiffness matrix becomes

$$\mathbf{k}_{i(P\Delta)} = \frac{EI}{L^3}\begin{bmatrix} 12 & 6L & -12 & 6L \\ 6L & 4L^2 & -6L & 2L^2 \\ -12 & -6L & 12 & -6L \\ 6L & 2L^2 & -6L & 4L^2 \end{bmatrix} + \frac{P}{L}\begin{bmatrix} -1 & 0 & 1 & 0 \\ 0 & 0 & 0 & 0 \\ 1 & 0 & -1 & 0 \\ 0 & 0 & 0 & 0 \end{bmatrix} \tag{30}$$

where $\mathbf{k}_{i(P\Delta)}$ is here known as the $P{-}\Delta$ stiffness of the member. While geometric nonlinearity due to sidesway can be captured using $\mathbf{k}_{i(P\Delta)}$ in Eq. 30, the magnification of response due to local deformation with an axial compressive force is totally ignored in one element model. But the $P{-}\delta$ effect of local deformation can be captured using several element $P{-}\Delta$ stiffnesses by subdividing the member into several elements in the model. The following example presents a simple illustration on the improvement of accuracy of $P{-}\Delta$ stiffness by subdividing a member into three elements. It also illustrates the consistencies of using stability functions in the formulation and the lack of consistencies in other element stiffness formulations.

Consider a member of length $3L$ with elastic modulus E and moment of inertia I subjected to an axial compressive force $P = 0.3 \times EI/L^2$ as shown in Fig. 4. No boundary condition needs to be applied to the member because only the element stiffness matrix is considered. Following Eqs. 18, 29, and 30, different forms of element stiffness matrices $\mathbf{k}_i$ using one long element with length $3L$ in the model with DOFs #1 to #4 can be written as

Layout: T1 Standard | Book ID: 330342_1_En | Book ISBN: 978-3-319-47796-1
Chapter No.: 6 | Date: 30-9-2016 Time: 7:37 pm | Page: 13/47

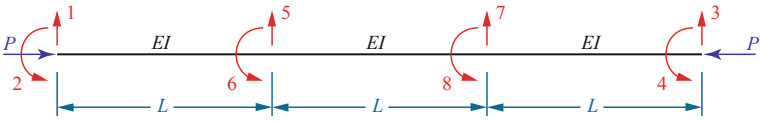

Fig. 4 Member subdivided into three elements

$$\mathbf{k}_{i(SF)} = \frac{EI}{L^3}\begin{bmatrix} 0.32405 & 0.63607L & -0.32405 & 0.63607L \\ 0.63607L & 1.20883L^2 & -0.63607L & 0.69938L^2 \\ -0.32405 & -0.63607L & 0.32405 & -0.63607L \\ 0.63607L & 0.69938L^2 & -0.63607L & 1.20883L^2 \end{bmatrix} \begin{matrix} \leftarrow \text{DOF\#1} \\ \leftarrow \text{DOF\#2} \\ \leftarrow \text{DOF\#3} \\ \leftarrow \text{DOF\#4} \end{matrix} \tag{31a}$$

$$\mathbf{k}_{i(GS)} = \frac{EI}{L^3}\begin{bmatrix} 0.32444 & 0.63667L & -0.32444 & 0.63667L \\ 0.63667L & 1.21333L^2 & -0.63667L & 0.69667L^2 \\ -0.32444 & -0.63667L & 0.32444 & -0.63667L \\ 0.63667L & 0.69667L^2 & -0.63667L & 1.21333L^2 \end{bmatrix} \begin{matrix} \leftarrow \text{DOF\#1} \\ \leftarrow \text{DOF\#2} \\ \leftarrow \text{DOF\#3} \\ \leftarrow \text{DOF\#4} \end{matrix} \tag{31b}$$

$$\mathbf{k}_{i(P\Delta)} = \frac{EI}{L^3}\begin{bmatrix} 0.34444 & 0.66667L & -0.34444 & 0.66667L \\ 0.66667L & 1.33333L^2 & -0.66667L & 0.66667L^2 \\ -0.34444 & -0.66667L & 0.34444 & -0.66667L \\ 0.66667L & 0.66667L^2 & -0.66667L & 1.33333L^2 \end{bmatrix} \begin{matrix} \leftarrow \text{DOF\#1} \\ \leftarrow \text{DOF\#2} \\ \leftarrow \text{DOF\#3} \\ \leftarrow \text{DOF\#4} \end{matrix} \tag{31c}$$

where $\mathbf{k}_{i(SF)}$ is the same as $\mathbf{k}_i$ in Eq. 18 but with the subscript '*SF*' added to denote that it is computed using the stability function method.

Now assume that the same member is subdivided into three elements of equal lengths L. The element stiffness matrices $\mathbf{k}_i$ with geometric nonlinearity for each of the three members are formulated, then by assembling each term into the global stiffness matrices according to DOFs #1 to #8 as labeled in Fig. 4, the final global stiffness matrices $\mathbf{K}_{SF}$, $\mathbf{K}_{GS}$, and $\mathbf{K}_{P\Delta}$ can be written as

$$\mathbf{K}_{SF} = \frac{EI}{L^3}\left[\begin{array}{cccc:cccc} 11.64 & 5.97L & 0 & 0 & -11.64 & 5.97L & 0 & 0 \\ 5.97L & 3.96L^2 & 0 & 0 & -5.97L & 2.01L^2 & 0 & 0 \\ 0 & 0 & 11.64 & -5.97L & 0 & 0 & -11.64 & -5.97L \\ 0 & 0 & -5.97L & 3.96L^2 & 0 & 0 & 5.97L & 2.01L^2 \\ \hdashline -11.64 & -5.97L & 0 & 0 & 23.28 & 0 & -11.64 & 5.97L \\ 5.97L & 2.01L^2 & 0 & 0 & 0 & 7.92L^2 & -5.97L & 2.01L^2 \\ 0 & 0 & -11.64 & 5.97L & -11.64 & -5.97L & 23.28 & 0 \\ 0 & 0 & -5.97L & 2.01L^2 & 5.97L & 2.01L^2 & 0 & 7.92L^2 \end{array}\right] \tag{32a}$$

Layout: T1 Standard | Book ID: 330342_1_En | Book ISBN: 978-3-319-47796-1
Chapter No.: 6 | Date: 30-9-2016 Time: 7:37 pm | Page: 14/47

$$\mathbf{K}_{GS} = \frac{EI}{L^3}\left[\begin{array}{cccc:cccc} 11.64 & 5.97L & 0 & 0 & -11.64 & 5.97L & 0 & 0 \\ 5.97L & 3.96L^2 & 0 & 0 & -5.97L & 2.01L^2 & 0 & 0 \\ 0 & 0 & 11.64 & -5.97L & 0 & 0 & -11.64 & -5.97L \\ 0 & 0 & -5.97L & 3.96L^2 & 0 & 0 & 5.97L & 2.01L^2 \\ \hdashline -11.64 & -5.97L & 0 & 0 & 23.28 & 0 & -11.64 & 5.97L \\ 5.97L & 2.01L^2 & 0 & 0 & 0 & 7.92L^2 & -5.97L & 2.01L^2 \\ 0 & 0 & -11.64 & 5.97L & -11.64 & -5.97L & 23.28 & 0 \\ 0 & 0 & -5.97L & 2.01L^2 & 5.97L & 2.01L^2 & 0 & 7.92L^2 \end{array}\right] \tag{32b}$$

$$\mathbf{K}_{P\Delta} = \frac{EI}{L^3}\left[\begin{array}{cccc:cccc} 11.7 & 6L & 0 & 0 & -11.7 & 6L & 0 & 0 \\ 6L & 4L^2 & 0 & 0 & -6L & 2L^2 & 0 & 0 \\ 0 & 0 & 11.7 & -6L & 0 & 0 & -11.7 & -6L \\ 0 & 0 & -6L & 4L^2 & 0 & 0 & 6L & 2L^2 \\ \hdashline -11.7 & -6L & 0 & 0 & 23.4 & 0 & -11.7 & 6L \\ 6L & 2L^2 & 0 & 0 & 0 & 8L^2 & -6L & 2L^2 \\ 0 & 0 & -11.7 & 6L & -11.7 & -6L & 23.4 & 0 \\ 0 & 0 & -6L & 2L^2 & 6L & 2L^2 & 0 & 8L^2 \end{array}\right] \begin{array}{l} \leftarrow \text{DOF\#1} \\ \leftarrow \text{DOF\#2} \\ \leftarrow \text{DOF\#3} \\ \leftarrow \text{DOF\#4} \\ \leftarrow \text{DOF\#5} \\ \leftarrow \text{DOF\#6} \\ \leftarrow \text{DOF\#7} \\ \leftarrow \text{DOF\#8} \end{array} \tag{32c}$$

where $\mathbf{K}_{SF}$, $\mathbf{K}_{GS}$, and $\mathbf{K}_{P\Delta}$ are the global stiffness matrices computed using the stability function method, geometric stiffness method, and $P-\Delta$ stiffness method, respectively.

Static condensation is now used to eliminate DOFs #5 to #8 from the global stiffness matrices in Eqs. 32a–32c based on the equation

$$\mathbf{K} = \left[\begin{array}{c:c} \mathbf{K}_{11} & \mathbf{K}_{12} \\ \hdashline \mathbf{K}_{21} & \mathbf{K}_{22} \end{array}\right], \qquad \overline{\mathbf{K}} = \mathbf{K}_{11} - \mathbf{K}_{12}\mathbf{K}_{22}^{-1}\mathbf{K}_{21} \tag{33}$$

where $\mathbf{K}_{11}$, $\mathbf{K}_{12}$, $\mathbf{K}_{21}$, and $\mathbf{K}_{22}$ are submatrices partitioned according to the dotted lines of those full stiffness matrices shown in Eqs. 32a–32c and 33, and $\overline{\mathbf{K}}$ represents the condensed global stiffness matrix. It can be seen that each of these submatrices is a 4×4 matrix, with subscript '2' denoting DOFs #5 to #8 to be eliminated and subscript '1' denoting DOFs #1 to #4 to remain after condensation. Now substituting these submatrices presented in Eqs. 32a–32c into Eq. 33 and performing the matrix multiplications gives

$$\overline{\mathbf{K}}_{SF} = \frac{EI}{L^3}\left[\begin{array}{cccc} 0.32405 & 0.63607L & -0.32405 & 0.63607L \\ 0.63607L & 1.20883L^2 & -0.63607L & 0.69938L^2 \\ -0.32405 & -0.63607L & 0.32405 & -0.63607L \\ 0.63607L & 0.69938L^2 & -0.63607L & 1.20883L^2 \end{array}\right] \begin{array}{l} \leftarrow \text{DOF\#1} \\ \leftarrow \text{DOF\#2} \\ \leftarrow \text{DOF\#3} \\ \leftarrow \text{DOF\#4} \end{array} \tag{34a}$$

Layout: T1 Standard | Book ID: 330342_1_En | Book ISBN: 978-3-319-47796-1
Chapter No.: 6 | Date: 30-9-2016 | Time: 7:37 pm | Page: 15/47

$$\overline{\mathbf{K}}_{GS} = \frac{EI}{L^3}\begin{bmatrix} 0.32410 & 0.63615L & -0.32410 & 0.63615L \\ 0.63615L & 1.20899L^2 & -0.63615L & 0.69945L^2 \\ -0.32410 & -0.63615L & 0.32410 & -0.63615L \\ 0.63615L & 0.69945L^2 & -0.63615L & 1.20899L^2 \end{bmatrix} \begin{matrix} \leftarrow \text{DOF\#1} \\ \leftarrow \text{DOF\#2} \\ \leftarrow \text{DOF\#3} \\ \leftarrow \text{DOF\#4} \end{matrix} \tag{34b}$$

$$\overline{\mathbf{K}}_{P\Delta} = \frac{EI}{L^3}\begin{bmatrix} 0.33429 & 0.65143L & -0.33429 & 0.65143L \\ 0.65143L & 1.24030L^2 & -0.65143L & 0.71399L^2 \\ -0.33429 & -0.65143L & 0.33429 & -0.65143L \\ 0.65143L & 0.71399L^2 & -0.65143L & 1.24030L^2 \end{bmatrix} \begin{matrix} \leftarrow \text{DOF\#1} \\ \leftarrow \text{DOF\#2} \\ \leftarrow \text{DOF\#3} \\ \leftarrow \text{DOF\#4} \end{matrix} \tag{34c}$$

Comparing the stiffness matrices in Eqs. 31a–31c using one-element formulation with those in Eqs. 34a–34c using three-element formulation shows that only the stability functions approach gives exactly the same stiffness matrix regardless of whether one long element is used or three subdivided elements are used (i.e., $\mathbf{k}_{i(SF)} = \overline{\mathbf{K}}_{SF}$, but $\mathbf{k}_{i(GS)} \approx \overline{\mathbf{K}}_{GS}$ and $\mathbf{k}_{i(P\Delta)} \neq \overline{\mathbf{K}}_{P\Delta}$). This indicates that while all three geometric nonlinearity approaches address large P–Δ appropriately, only the stability functions approach consistently captures the small P–δ effect. Note that the difference between $\mathbf{k}_{i(P\Delta)}$ in Eq. 31c and $\mathbf{k}_{i(SF)}$ in Eq. 31a is quite significant, but the difference becomes smaller when $\overline{\mathbf{K}}_{P\Delta}$ in Eq. 34c is compared to $\overline{\mathbf{K}}_{SF}$ in Eq. 34a. This indicates that capturing small P–δ effect using the P–Δ stiffness matrix is possible by subdividing the member into several elements, but it also indicates that subdividing into three elements at an axial compressive force of $P = 0.3 \times EI/L^2$ is insufficient to capture the small P–δ effect using the P–Δ stiffness matrix only.

4 Nonlinear Static Analysis of Framed Structures

Once the global stiffness matrices $\mathbf{K}$, $\mathbf{K}'$, and $\mathbf{K}''$ in Eqs. 28a–28c are assembled from the element stiffness matrices $\mathbf{k}_i$, $\mathbf{k}'_i$, and $\mathbf{k}''_i$ in Eqs. 18, 24, and 27, respectively, they can be used to perform static analysis of moment-resisting framed structures with both geometric and material nonlinearities. For the structure modeled as a multi-degree of freedom (MDOF) system, the derivation of the analysis procedure begins with the concept of inelastic displacements. Considering a structure having n DOFs, the displacement can be written in vector form as

$$\mathbf{x} = \mathbf{x}' + \mathbf{x}'' = \begin{Bmatrix} x'_1 \\ x'_2 \\ \vdots \\ x'_n \end{Bmatrix} + \begin{Bmatrix} x''_1 \\ x''_2 \\ \vdots \\ x''_n \end{Bmatrix} \tag{35}$$

Layout: T1 Standard | Book ID: 330342_1_En | Book ISBN: 978-3-319-47796-1
Chapter No.: 6 | Date: 30-9-2016 Time: 7:37 pm | Page: 16/47

where x represents the total displacement vector, $\mathbf{x}'$ is the elastic displacement vector, and $\mathbf{x}''$ is the inelastic displacement vector. For moment-resisting framed structures, let the total moment vector $\mathbf{M}$ at the plastic hinge locations (PHLs) be described in vector form as

$$\mathbf{M} = \mathbf{M}' + \mathbf{M}'' = \begin{Bmatrix} M_1' \\ M_2' \\ \vdots \\ M_m' \end{Bmatrix} + \begin{Bmatrix} M_1'' \\ M_2'' \\ \vdots \\ M_m'' \end{Bmatrix} \tag{36}$$

where $\mathbf{M}'$ is the elastic moment vector due to elastic displacement $\mathbf{x}'$, and $\mathbf{M}''$ is the inelastic moment vector due to inelastic displacement $\mathbf{x}''$ that is caused by plastic rotations. The value m represents the total number of PHLs in the moment-resisting frame.

4.1 Residual Components Due to Plastic Rotations

Consider first the inelastic moment vector $\mathbf{M}''$ that is caused by plastic rotations in the moment-resisting frame. Define the plastic rotation vector $\boldsymbol{\Theta}''$ as

$$\boldsymbol{\Theta}'' = \begin{Bmatrix} \theta_1'' \\ \theta_2'' \\ \vdots \\ \theta_m'' \end{Bmatrix} \tag{37}$$

An example of having plastic rotations developed at two PHLs of the ith member is shown in Fig. 5a. This state of the structure can never exist because this member violates either the compatibility or the equilibrium condition with the adjacent joints. Without any force applied to this member, it should remain straight, yet the plastic rotations induce incompatibility with the adjacent joints that have no rotation. On the other hand, if the member is deformed in a compatible way with the adjacent joint, forces must be applied to this member resulting in violation of the equilibrium condition of the joint. To ensure the member deforms in a compatible way with the rest of the structure while satisfying the equilibrium condition, this member with plastic rotations $\boldsymbol{\Theta}''$ is first isolated from the structure and restoring forces are applied to restore this member back to the original undeformed shape, as shown in Fig. 5b. This induces internal restoring forces $\mathbf{F}_{RF}$ and the fixed-end shears and moments on the member. At the global degree of freedom level, the restoring force is an $n \times 1$ vector of the form:

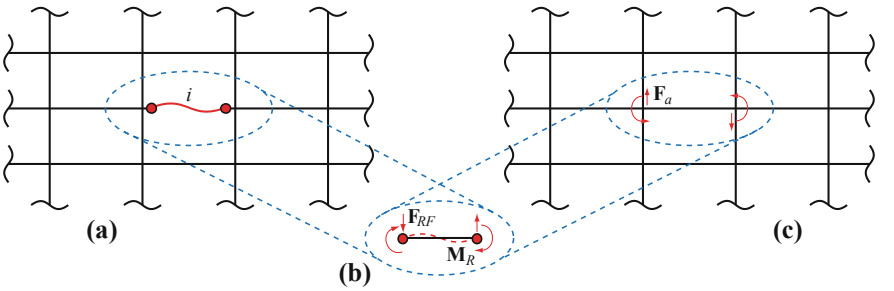

Fig. 5 Satisfying compatibility and equilibrium conditions in nonlinear static analysis

$$\mathbf{F}_{RF} = \begin{Bmatrix} F_{RF1} \\ F_{RF2} \\ \vdots \\ F_{RFn} \end{Bmatrix} = -\mathbf{K}'\boldsymbol{\Theta}'' \tag{38}$$

where $\mathbf{K}'$ is the $n \times m$ assembled global stiffness matrix defined in Eq. 28b. In addition to the restoring forces $\mathbf{F}_{RF}$ that are applied at the global DOFs, plastic rotations $\boldsymbol{\Theta}''$ induce residual moments $\mathbf{M}_R$ at the PHLs as shown in Fig. 5b. At the local PHL, the residual moment is an $m \times 1$ vector in the form:

$$\mathbf{M}_R = \begin{Bmatrix} M_{R,1} \\ M_{R,2} \\ \vdots \\ M_{R,m} \end{Bmatrix} = -\mathbf{K}''\boldsymbol{\Theta}'' \tag{39}$$

where $\mathbf{K}''$ is the $m \times m$ global stiffness matrix defined in Eq. 28c. The minus signs appear in Eqs. 38 and 39 because negative actions must be applied in order to rotate a positive plastic rotation back to zero, which results in negative restoring forces and negative residual moments.

Now the member is assembled back into the structure and the deformation of this *i*th member is compatible with the rest of the structure. However, the restoring forces $\mathbf{F}_{RF}$ as shown in Fig. 5b are actually not present globally as shown in Fig. 5a, and as a result equal and opposite forces $\mathbf{F}_a = -\mathbf{F}_{RF}$ must be applied to the structure's DOFs to cancel these restoring forces, as shown in Fig. 5c. Substituting Eq. 38 into the equation gives

$$\mathbf{F}_a = -\mathbf{F}_{RF} = \mathbf{K}'\boldsymbol{\Theta}'' \tag{40}$$

Applying the equivalent forces $\mathbf{F}_a$ results in a permanent deformation of the structure, which is exactly the inelastic displacement $\mathbf{x}''$. The relationship can be obtained through conducting the matrix structural analysis for MDOF systems as:

Layout: T1 Standard | Book ID: 330342_1_En | Book ISBN: 978-3-319-47796-1
Chapter No.: 6 | Date: 30-9-2016 Time: 7:37 pm | Page: 18/47

$$\mathbf{F}_a = \mathbf{K}\mathbf{x}'' \tag{41}$$

where $\mathbf{K}$ is the $n \times n$ global stiffness matrix defined in Eq. 28a. Through this process, the structure remains in equilibrium in addition to being compatible. Equating $\mathbf{F}_a$ in both Eqs. 40 and 41 and solving for the inelastic displacements $\mathbf{x}''$ gives

$$\mathbf{x}'' = \mathbf{K}^{-1}\mathbf{K}'\boldsymbol{\Theta}'' \tag{42}$$

Due to the induced equivalent forces $\mathbf{F}_a$, which produce inelastic displacements $\mathbf{x}''$ in the structure, additional moments are also induced at the PHLs. Denoting this induced moment vector as $\mathbf{M}_P$, it is related to the inelastic displacement $\mathbf{x}''$ by the equation

$$\mathbf{M}_P = \mathbf{K}'^T\mathbf{x}'' \tag{43}$$

where $\mathbf{K}'^T$ is the transpose of the $\mathbf{K}'$ matrix in Eq. 28b. Then substituting Eq. 42 into Eq. 43 gives

$$\mathbf{M}_P = \mathbf{K}'^T\mathbf{K}^{-1}\mathbf{K}'\boldsymbol{\Theta}'' \tag{44}$$

Finally, the inelastic moment vector $\mathbf{M}''$ at the PHLs in Fig. 5a is determined by summing the residual moments $\mathbf{M}_R$ at the PHLs shown in Fig. 5b and the induced moments $\mathbf{M}_P$ shown in Fig. 5c, i.e.,

$$\mathbf{M}'' = \mathbf{M}_R + \mathbf{M}_P \tag{45}$$

Substituting Eqs. 39 and 44 into Eq. 45 gives the equation for inelastic moments $\mathbf{M}''$ as a function of plastic rotations $\boldsymbol{\Theta}''$:

$$\mathbf{M}'' = -\left(\mathbf{K}'' - \mathbf{K}'^T\mathbf{K}^{-1}\mathbf{K}'\right)\boldsymbol{\Theta}'' \tag{46}$$

Equations 42 and 46 represent the inelastic displacement and inelastic moment vectors due to the plastic rotations within the structure with no externally applied force. This can be interpreted as the case when an earthquake causes plastic rotations within the structure, then the inelastic displacements represent the permanent deformation (or sometimes known as the residual drift) of the structure and inelastic moments represent the forces remaining in the members after the earthquake motion subsides.

4.2 Elastic Components Due to Elastic Displacements

Now consider the relationship between the elastic moments $\mathbf{M}'$ and the elastic displacements $\mathbf{x}'$ due to the external applied static load $\mathbf{F}_o$. Similar to Eq. 41 where

Layout: T1 Standard | Book ID: 330342_1_En | Book ISBN: 978-3-319-47796-1
Chapter No.: 6 | Date: 30-9-2016 | Time: 7:37 pm | Page: 19/47

the inelastic displacements $\mathbf{x}''$ are due to the application of the induced equivalent loads $\mathbf{F}_a$, the elastic displacements $\mathbf{x}'$ of the structure are the result of applying the external static loads $\mathbf{F}_o$. Again by using the matrix structural analysis for multi-degree of freedom systems, the external static loads $\mathbf{F}_o$ are related to the elastic displacements $\mathbf{x}'$ through the $n \times n$ global stiffness matrix $\mathbf{K}$, i.e.,

$$\mathbf{F}_o = \mathbf{K}\mathbf{x}' \tag{47}$$

Similarly from Eq. 43, where the induced moments $\mathbf{M}_P$ are related to the inelastic displacements $\mathbf{x}''$ due to the application of the induced equivalent load $\mathbf{F}_a$, the elastic moments $\mathbf{M}'$ are related to the elastic displacements $\mathbf{x}'$ through the $\mathbf{K}'^T$ matrix, i.e.,

$$\mathbf{M}' = \mathbf{K}'^T\mathbf{x}' \tag{48}$$

4.3 Analysis Procedure Using Total Responses

Once the elastic and inelastic portions of the structures are characterized, the objective now is to apply Eqs. 35 and 36 and represent the analytical procedure using the total displacements $\mathbf{x}$, total moments $\mathbf{M}$, plastic rotation $\boldsymbol{\Theta}''$, and the external applied static load $\mathbf{F}_o$. Equation 35 is first considered by solving for the elastic displacements $\mathbf{x}'$, i.e., $\mathbf{x}' = \mathbf{x} - \mathbf{x}''$, and substituting this result into Eqs. 47 and 48 gives

$$\mathbf{F}_o = \mathbf{K}[\mathbf{x} - \mathbf{x}''], \quad \mathbf{M}' = \mathbf{K}'^T[\mathbf{x} - \mathbf{x}''] \tag{49}$$

Then substituting the inelastic displacements $\mathbf{x}''$ in Eq. 42 into Eq. 49 gives

$$\mathbf{F}_o = \mathbf{K}\left[\mathbf{x} - \mathbf{K}^{-1}\mathbf{K}'\boldsymbol{\Theta}''\right], \quad \mathbf{M}' = \mathbf{K}'^T\left[\mathbf{x} - \mathbf{K}^{-1}\mathbf{K}'\boldsymbol{\Theta}''\right] \tag{50}$$

Simplifying the first equation of Eq. 50 gives

$$\mathbf{F}_o = \mathbf{K}\mathbf{x} - \mathbf{K}'\boldsymbol{\Theta}'' \tag{51}$$

Now based on Eq. 36, the total moment vector $\mathbf{M}$ at all the PHLs is calculated by substituting the elastic moments $\mathbf{M}'$ in Eq. 50 and the inelastic moments $\mathbf{M}''$ in Eq. 46 in the equation. Doing so gives

$$\mathbf{M} = \mathbf{M}' + \mathbf{M}'' = \mathbf{K}'^T\left[\mathbf{x} - \mathbf{K}^{-1}\mathbf{K}'\boldsymbol{\Theta}''\right] - \left[\mathbf{K}'' - \mathbf{K}'^T\mathbf{K}^{-1}\mathbf{K}'\right]\boldsymbol{\Theta}'' = \mathbf{K}'^T\mathbf{x} - \mathbf{K}''\boldsymbol{\Theta}'' \tag{52}$$

Layout: T1 Standard | Book ID: 330342_1_En | Book ISBN: 978-3-319-47796-1
Chapter No.: 6 | Date: 30-9-2016 | Time: 7:37 pm | Page: 20/47

Combining Eqs. 51 and 52 gives the governing equation of the analysis procedure for solving nonlinear static problems:

$$\left[\begin{array}{c|c} \mathbf{K} & \mathbf{K}' \\ \hline \mathbf{K}'^{T} & \mathbf{K}'' \end{array}\right]\left\{\begin{array}{c} \mathbf{x} \\ \hline -\boldsymbol{\Theta}'' \end{array}\right\}=\left\{\begin{array}{c} \mathbf{F}_o \\ \hline \mathbf{M} \end{array}\right\} \tag{53}$$

Equation 53 shows both the $n \times 1$ total displacement vector $\mathbf{x}$ (n unknowns for the DOFs) and the $m \times 1$ plastic rotation vector $\boldsymbol{\Theta}''$ (m unknowns for the PHLs) make up the unknown vector that is typically required to be solved in the nonlinear structural analysis problem. However, because material nonlinearity is involved in this equation, the solution requires performing an iterative procedure. To illustrate this iterative procedure, the goal is to solve for the unknowns $\mathbf{x}$, $\boldsymbol{\Theta}''$, and $\mathbf{M}$ for any applied static force pattern $\mathbf{F}_o$. This adds up to a total of $n+2m$ unknowns, and therefore the solution requires $n+2m$ equations provided as follows:

- Equation 53 by itself gives $n+m$ independent equations that satisfy both global equilibrium and compatibility conditions.
- Each plastic hinge contains its own moment versus plastic rotation relationship, which gives additional m equations that follows the local hysteretic behavior of the plastic hinges.

Using these $n+2m$ equations, the $n+2m$ unknowns (i.e., $\mathbf{x}$, $\boldsymbol{\Theta}''$, and $\mathbf{M}$) in Eq. 53 can be solved uniquely. Once these unknowns are calculated, the inelastic displacements $\mathbf{x}''$ can be determined using Eq. 42. This completes the calculations for the nonlinear static analysis.

4.4 Implementation of the Analysis Procedure with Updates to Geometric Nonlinearity

The following example is used to illustrate the procedure for statically analyzing moment-resisting framed structure with geometric and material nonlinearities. Consider a one-story one-bay moment-resisting steel frame shown in Fig. 6. Assume that axial deformation is ignored for all three members, this results in a system with 3 DOFs ($n=3$) and 6 PHLs ($m=6$) as labeled in the figure. Also assume that a lateral force of F_o is applied at x_1. This gives $F_1 = F_o$ and $F_2 = F_3 = 0$, and therefore

$$\mathbf{F}_o = \left\{\begin{array}{c} F_1 \\ F_2 \\ F_3 \end{array}\right\} = \left\{\begin{array}{c} F_o \\ 0 \\ 0 \end{array}\right\} \tag{54}$$

Let the gravity load on the frame be $P = 890$ kN and the lengths of the members be $L_b = 6.10$ m and $L_c = 4.27$ m. For W14 $\times$ 82 columns, the cross-sectional area

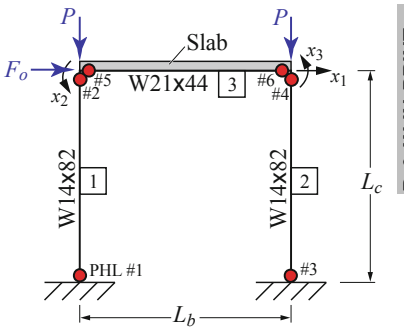

Fig. 6 One-story one-bay moment-resisting steel frame

is $A_c = 15,500$ mm^2, the moment of inertia is $I_c = 3.67 \times 10^8$ mm^4, and the plastic section modulus is $Z_c = 2,278,000$ mm^3. For the W21 × 44 beam, the moment of inertia is $I_b = 3.47 \times 10^8$ mm^4, and the plastic section modulus is $Z_b = 1,876,000$ mm^3, while the cross-sectional area of the beam is not used in the calculation. A elastic modulus of $E = 200$ GPa and a yield stress of $f_Y = 248$ MPa for steel are used.

Since the axial force in Member 1 (denoted as P_1) will be different from that of Member 2 (denoted as P_2) due to overturning induced by the lateral applied force F_o, the resulting stability coefficients will be different as well. The axial force in Member 3 is assumed to be negligible (i.e., $P_3 \approx 0$) due to the presence of slab. Therefore, let

$$\lambda_1 = \sqrt{P_1/EI_c} \times L_c, \quad \lambda_2 = \sqrt{P_2/EI_c} \times L_c \tag{55}$$

It follows that the global stiffness matrices for this one-story frame become:

$$\mathbf{K} = \begin{bmatrix} s_1' EI_c/L_c^3 + s_2' EI/L_c^3 & \bar{s}_1 EI_c/L_c^2 & \bar{s}_2 EI_c/L_c^2 \\ \bar{s}_1 EI_c/L_c^2 & s_1 EI_c/L_c + 4EI_b/L_b & 2EI_b/L_b \\ \bar{s}_2 EI_c/L_c^2 & 2EI_b/L_b & s_2 EI_c/L_c + 4EI_b/L_b \end{bmatrix} \begin{matrix} \leftarrow x_1 \\ \leftarrow x_2 \\ \leftarrow x_3 \end{matrix} \tag{56a}$$

$$\mathbf{K}' = \left[\begin{array}{cc|cc|cc} \bar{s}_1 EI_c/L_c^2 & \bar{s}_1 EI_c/L_c^2 & \bar{s}_2 EI_c/L_c^2 & \bar{s}_2 EI_c/L_c^2 & 0 & 0 \\ s_1 c_1 EI_c/L_c & s_1 EI_c/L_c & 0 & 0 & 4EI_b/L_b & 2EI_b/L_b \\ 0 & 0 & s_2 c_2 EI_c/L_c & s_2 EI_c/L_c & 2EI_b/L_b & 4EI_b/L_b \end{array}\right] \begin{matrix} \leftarrow x_1 \\ \leftarrow x_2 \\ \leftarrow x_3 \end{matrix} \tag{56b}$$

$$\mathbf{K}'' = \left[\begin{array}{cc|cc|cc} s_1 EI_c/L_c & s_1 c_1 EI_c/L_c & 0 & 0 & 0 & 0 \\ s_1 c_1 EI_c/L_c & s_1 EI_c/L_c & 0 & 0 & 0 & 0 \\ \hline 0 & 0 & s_2 EI_c/L_c & s_2 c_2 EI_c/L_c & 0 & 0 \\ 0 & 0 & s_2 c_2 EI_c/L_c & s_2 EI_c/L_c & 0 & 0 \\ \hline 0 & 0 & 0 & 0 & 4EI_b/L_b & 2EI_b/L_b \\ 0 & 0 & 0 & 0 & 2EI_b/L_b & 4EI_b/L_b \end{array}\right] \begin{matrix} \leftarrow \theta_1'' \\ \leftarrow \theta_2'' \\ \leftarrow \theta_3'' \\ \leftarrow \theta_4'' \\ \leftarrow \theta_5'' \\ \leftarrow \theta_6'' \end{matrix} \tag{56c}$$

Layout: T1 Standard | Book ID: 330342_1_En | Book ISBN: 978-3-319-47796-1
Chapter No.: 6 | Date: 30-9-2016 Time: 7:37 pm | Page: 22/47

where s_1, c_1, $\bar{s}_1$, and s_1' are the stability coefficients of Member 1 as functions of λ_1 and P_1, and s_2, c_2, $\bar{s}_2$, and s_2' are the stability coefficients of Member 2 as functions of λ_2 and P_2. Then Eq. 53 becomes

$$\left[\begin{array}{c|c} \mathbf{K}(3\times3) & \mathbf{K}'(3\times6) \\ \hline \mathbf{K}'^{T}(6\times3) & \mathbf{K}''(6\times6) \end{array}\right] \left\{\begin{array}{c} x_1 \\ x_2 \\ x_3 \\ \hline -\theta_1'' \\ -\theta_2'' \\ -\theta_3'' \\ -\theta_4'' \\ -\theta_5'' \\ -\theta_6'' \end{array}\right\} = \left\{\begin{array}{c} F_o \\ 0 \\ 0 \\ \hline M_1 \\ M_2 \\ M_3 \\ M_4 \\ M_5 \\ M_6 \end{array}\right\} \tag{57}$$

The yielding characteristics of each plastic hinge must also be defined. Assume the material exhibits elastic-plastic behavior, and an elliptical yield surface is used with the interaction between axial force and moment of the column and beam members following the relationships:

$$\text{Columns}: \left(\frac{P_k}{f_Y A_c}\right)^2 + \left(\frac{M_k}{f_Y Z_c}\right)^2 \le 1, \quad k = 1,\ldots,4 \tag{58a}$$

$$\text{Beam}: \left|\frac{M_k}{f_Y Z_b}\right| \le 1, \quad k = 5,6 \tag{58b}$$

Following Eqs. 58a, 58b, this gives the moment versus plastic rotation relationships for the 6 PHLs as

$$\text{if} \begin{cases} M_k \le M_{Yc,k} \\ M_k > M_{Yc,k} \end{cases}, \quad \text{then} \quad \begin{cases} \theta_k'' = 0 \\ M_k = M_{Yc,k} \end{cases} \quad i = 1,2,3,4 \tag{59a}$$

$$\text{if} \begin{cases} M_i \le f_Y Z_b \\ M_i > f_Y Z_b \end{cases}, \quad \text{then} \quad \begin{cases} \theta_i'' = 0 \\ M_i = f_Y Z_b \end{cases} \quad i = 5,6 \tag{59b}$$

where $M_{Yc,k}$ is the moment capacity of the kth column plastic hinge computed based on a specified axial compressive force and the yield surface equation given in Eq. 58a.

To demonstrate the nonlinear static analysis procedure using the currently proposed improved method, a pushover curve is now constructed for the frame by taking the following steps.

Step U1: The frame is initially assumed to respond in the linearly elastic range i.e., $\theta_1'' = \theta_2'' = \theta_3'' = \theta_4'' = \theta_5'' = \theta_6'' = 0$. At an applied force of $F_o = 414.8$ kN and $P_1 = P_2 = 890$ kN, extracting the first three equations of Eq. 57 gives

Layout: T1 Standard | Book ID: 330342_1_En | Book ISBN: 978-3-319-47796-1
Chapter No.: 6 | Date: 30-9-2016 Time: 7:37 pm | Page: 23/47

$$\begin{bmatrix} 22145 & 24069 & 24069 \\ 24069 & 114253 & 23017 \\ 24069 & 23017 & 114253 \end{bmatrix} \begin{Bmatrix} x_1 \\ x_2 \\ x_3 \end{Bmatrix} = \begin{Bmatrix} 414.8 \\ 0 \\ 0 \end{Bmatrix} \tag{60}$$

Solving for the displacements at the DOFs gives

$$x_1 = 0.0303\,\text{m}, \quad x_2 = x_3 = -0.00531\,\text{rad} \tag{61}$$

Then substituting the results in Eq. 61 back into the last six equations of Eq. 57 gives the moments

$$\begin{Bmatrix} M_1 \\ M_2 \\ M_3 \\ M_4 \\ M_5 \\ M_6 \end{Bmatrix} = \begin{bmatrix} 24069 & 34491 & 0 \\ 24069 & 68219 & 0 \\ 24069 & 0 & 34491 \\ 24069 & 0 & 68219 \\ 0 & 46034 & 23017 \\ 0 & 23017 & 46034 \end{bmatrix} \begin{Bmatrix} 0.0303 \\ -0.00531 \\ -0.00531 \end{Bmatrix} = \begin{Bmatrix} 545.5 \\ 366.5 \\ 545.5 \\ 366.5 \\ -366.5 \\ -366.5 \end{Bmatrix} \tag{62}$$

Based on the setup of the frame as shown in Fig. 5, the column axial forces are determined by computing the shear forces at the two ends of the beam member by using equilibrium of the beam and directly transfer to the columns, i.e.,

$$P_1 = P + (M_5 + M_6)/L_b = 890 + (-366.5 - 366.5)/6.10 = 769\,\text{kN} \tag{63a}$$

$$P_2 = P - (M_5 + M_6)/L_b = 890 - (-366.5 - 366.5)/6.10 = 1010\,\text{kN} \tag{63b}$$

Then using Eq. 59a to check for yielding at PHLs #1 and #3 gives

$$\text{PHL } \#1: \ (769/3843)^2 + (545.5/565.4)^2 = 0.971 \tag{64a}$$

$$\text{PHL } \#3: \ (1010/3843)^2 + (545.5/565.4)^2 = 1.000 \tag{64b}$$

which indicates that PHL #3 reaches its yield surface, where any additional loading will cause yielding at this plastic hinge.

Step U2: The analysis continues with PHL #3 yielded, i.e., $\theta_1'' = \theta_2'' = \theta_4'' = \theta_5'' = \theta_6'' = 0$. The lateral force is applied up to $F_o = 418.7$ kN. Rows 1, 2, 3, and 6 are extracted from Eq. 57 with updated geometric nonlinearity based on the column axial forces obtained in Eqs. 63a, 63b:

$$\left[\begin{array}{ccc:c} 22145 & 24082 & 24057 & 24057 \\ 24082 & 114322 & 23017 & 0 \\ 24057 & 23017 & 114184 & 34508 \\ \hdashline 24057 & 0 & 34508 & 68150 \end{array}\right] \left\{\begin{array}{c} x_1 \\ x_2 \\ x_3 \\ \hdashline -\theta_3'' \end{array}\right\} = \left\{\begin{array}{c} 418.7 \\ 0 \\ 0 \\ \hdashline 545.5 \end{array}\right\} \tag{65}$$

Solving for the displacements at the DOFs and plastic rotations in Eq. 65 gives

$$x_1 = 0.0307\,\text{m}, \quad x_2 = -0.00540\,\text{rad}, \quad x_3 = -0.00535\,\text{rad}, \quad \theta_3'' = 0.00014\,\text{rad} \tag{66}$$

Then substituting the results in Eq. 66 back into the last six equations of Eq. 57 gives the moments

$$\begin{Bmatrix} M_1 \\ M_2 \\ M_3 \\ M_4 \\ M_5 \\ M_6 \end{Bmatrix} = \left[\begin{array}{cccc:c} 24082 & 34473 & 0 & 0 & \\ 24082 & 68288 & 0 & 0 & \\ 24057 & 0 & 34508 & 68150 & \\ 24057 & 0 & 68150 & 34508 & \\ 0 & 46034 & 23017 & 0 & \\ 0 & 23017 & 46034 & 0 & \end{array}\right] \left\{\begin{array}{c} 0.0307 \\ -0.00540 \\ \hdashline -0.00535 \\ -0.00014 \end{array}\right\} = \begin{Bmatrix} 554.0 \\ 371.5 \\ 545.5 \\ 370.3 \\ -371.5 \\ -370.3 \end{Bmatrix} \tag{67}$$

and the column axial forces are updated as

$$P_1 = P + (M_5 + M_6)/L_b = 890 + (-371.5 - 370.3)/6.10 = 768\,\text{kN} \tag{68a}$$

$$P_2 = P - (M_5 + M_6)/L_b = 890 - (-371.5 - 370.3)/6.10 = 1011\,\text{kN} \tag{68b}$$

Then using Eq. 59a to check for yielding at PHLs #1 and #3 gives

$$\text{PHL } \#1: \ (768/3843)^2 + (554.0/565.4)^2 = 1.000 \tag{69a}$$

$$\text{PHL } \#3: \ (1011/3843)^2 + (545.5/565.4)^2 = 1.000 \tag{69b}$$

which indicates that PHL #1 reaches its capacity and PHL #3 continues yielding at this step.

Step U3: The analysis continues with PHLs #1 and #3 yielded, i.e., $\theta_2'' = \theta_4'' = \theta_5'' = \theta_6'' = 0$. The lateral force is applied up to $F_o = 457.0$ kN. Rows 1, 2, 3, 4, and 6 are extracted from Eq. 57 with updated geometric nonlinearity based on the column axial forces obtained in Eqs. 68a, 68b:

$$\left[\begin{array}{ccc:cc} 22145 & 24082 & 24057 & 24082 & 24057 \\ 24082 & 114323 & 23017 & 34473 & 0 \\ 24057 & 23017 & 114183 & 0 & 34508 \\ \hdashline 24082 & 34473 & 0 & 68289 & 0 \\ 24057 & 0 & 34508 & 0 & 68150 \end{array}\right] \left\{\begin{array}{c} x_1 \\ x_2 \\ x_3 \\ \hdashline -\theta_1'' \\ -\theta_3'' \end{array}\right\} = \left\{\begin{array}{c} 457.0 \\ 0 \\ 0 \\ \hdashline 554.0 \\ 545.5 \end{array}\right\} \tag{70}$$

Solving for the displacements at the DOFs and plastic rotations in Eq. 70 gives

Layout: T1 Standard | Book ID: 330342_1_En | Book ISBN: 978-3-319-47796-1
Chapter No.: 6 | Date: 30-9-2016 Time: 7:37 pm | Page: 25/47

$$x_1 = 0.0445\,\text{m}, \quad x_2 = -0.00676\,\text{rad}, \quad x_3 = -0.00671\,\text{rad}$$

$$\theta_1'' = 0.00415\,\text{rad}, \quad \theta_3'' = 0.00429\,\text{rad} \tag{71}$$

Then substituting the results in Eq. 71 back into the last six equations of Eq. 57 gives the moments

$$\begin{Bmatrix} M_1 \\ M_2 \\ M_3 \\ M_4 \\ M_5 \\ M_6 \end{Bmatrix} = \left[\begin{array}{ccc:cc:c} 24082 & 34473 & 0 & 68289 & 0 & \\ 24082 & 68289 & 0 & 34473 & 0 & \\ 24057 & 0 & 34508 & 0 & 68150 & \\ 24057 & 0 & 68150 & 0 & 34508 & \\ 0 & 46034 & 23017 & 0 & 0 & \\ 0 & 23017 & 46034 & 0 & 0 & \end{array}\right] \left\{\begin{array}{c} 0.0445 \\ -0.00676 \\ -0.00671 \\ \hdashline -0.00415 \\ -0.00429 \end{array}\right\} = \left\{\begin{array}{c} 553.9 \\ 465.6 \\ 545.4 \\ 464.3 \\ -465.6 \\ -464.3 \end{array}\right\} \tag{72}$$

At this point, the moment at PHL #5 reaches its capacity of $f_Y Z_b = 465.6$ kN-m, and the column axial forces are updated as

$$P_1 = P + (M_5 + M_6)/L_b = 890 + (-465.6 - 464.3)/6.10 = 737\,\text{kN} \tag{73a}$$

$$P_2 = P - (M_5 + M_6)/L_b = 890 - (-465.6 - 464.3)/6.10 = 1042\,\text{kN} \tag{73b}$$

Step U4: The analysis continues with PHLs #1, #3, and #5 yielded, i.e., $\theta_2'' = \theta_4'' = \theta_6'' = 0$. The lateral force is applied up to $F_o = 457.1$ kN. Rows 1, 2, 3, 4, 6, and 8 are extracted from Eq. 57 with updated geometric nonlinearity based on the column axial forces obtained in Eqs. 73a, 73b:

$$\left[\begin{array}{ccc:ccc} 22145 & 24085 & 24054 & 24085 & 24054 & 0 \\ 24085 & 114340 & 23017 & 34469 & 0 & 46034 \\ 24054 & 23017 & 114166 & 0 & 34513 & 23017 \\ \hdashline 24085 & 34469 & 0 & 68306 & 0 & 0 \\ 24054 & 0 & 34513 & 0 & 68132 & 0 \\ 0 & 46034 & 23017 & 0 & 0 & 46034 \end{array}\right] \left\{\begin{array}{c} x_1 \\ x_2 \\ x_3 \\ \hdashline -\theta_1'' \\ -\theta_3'' \\ -\theta_5'' \end{array}\right\} = \left\{\begin{array}{c} 457.1 \\ 0 \\ 0 \\ \hdashline 553.9 \\ 545.4 \\ -465.6 \end{array}\right\} \tag{74}$$

Solving for the displacements at the DOFs and plastic rotations in Eq. 70 gives

$$x_1 = 0.0448\,\text{m}, \quad x_2 = -0.00685\,\text{rad}, \quad x_3 = -0.00674\,\text{rad}$$

$$\theta_1'' = 0.00421\,\text{rad}, \quad \theta_3'' = 0.00441\,\text{rad}, \quad \theta_5'' = -0.00011\,\text{rad} \tag{75}$$

Then substituting the results in Eq. 75 back into the last six equations of Eq. 57 gives the moments

$$\begin{Bmatrix} M_1 \\ M_2 \\ M_3 \\ M_4 \\ M_5 \\ M_6 \end{Bmatrix} = \left[\begin{array}{ccc:ccc} 24085 & 34469 & 0 & 68306 & 0 & 0 \\ 24085 & 68306 & 0 & 34469 & 0 & 0 \\ 24054 & 0 & 34513 & 0 & 68134 & 0 \\ 24054 & 0 & 68132 & 0 & 34513 & 0 \\ 0 & 46034 & 23017 & 0 & 0 & 46034 \\ 0 & 23017 & 46034 & 0 & 0 & 23017 \end{array}\right] \begin{Bmatrix} 0.0448 \\ -0.00685 \\ -0.00674 \\ -0.00421 \\ -0.00441 \\ 0.00011 \end{Bmatrix} = \begin{Bmatrix} 554.9 \\ 465.6 \\ 544.2 \\ 465.6 \\ -465.6 \\ -465.6 \end{Bmatrix} \tag{76}$$

At this point, the moment at PHL #6 reaches its capacity of $f_Y Z_b = 465.6$ kN-m, and the column axial forces are updated as

$$P_1 = P + (M_5 + M_6)/L_b = 890 + (-465.6 - 465.6)/6.10 = 737\,\text{kN} \tag{77a}$$

$$P_2 = P - (M_5 + M_6)/L_b = 890 - (-465.6 - 465.6)/6.10 = 1042\,\text{kN} \tag{77b}$$

Step U5: Now that a mechanism has developed with the formation of plastic hinges at PHLs #1, #3, #5, and #6, the frame will continue to deflect without any additional load. But as the displacement increases, the gravity loads of $P = 890$ kN cause an increase in column moments due to P–Δ effect, resulting in a reduction of the amount of lateral load that can be withstood by the frame. This effect can be captured easily in the current analysis procedure. Let the analysis continue with PHLs #1, #3, #5, and #6 yielded, i.e., $\theta_2'' = \theta_4'' = 0$. By using any applied lateral force less than $F_o = 457.1$ kN (from Step U4) to capture the lateral load reduction, say $F_o = 434.1$ kN, Rows 1, 2, 3, 4, 6, 8, and 9 are extracted from Eq. 57 with updated geometric nonlinearity based on the column axial forces obtained in Eqs. 77a, 77b:

$$\left[\begin{array}{ccc:ccc} 22145 & 24085 & 24054 & 24085 & 24054 & 0 & 0 \\ 24085 & 114340 & 23017 & 34469 & 0 & 46034 & 23017 \\ 24054 & 23017 & 114165 & 0 & 34513 & 23017 & 46034 \\ \hdashline 24085 & 34469 & 0 & 68307 & 0 & 0 & 0 \\ 24054 & 0 & 34513 & 0 & 68132 & 0 & 0 \\ 0 & 46034 & 23017 & 0 & 0 & 46034 & 23017 \\ 0 & 23017 & 46034 & 0 & 0 & 23017 & 46034 \end{array}\right] \begin{Bmatrix} x_1 \\ x_2 \\ x_3 \\ \hdashline -\theta_1'' \\ -\theta_3'' \\ -\theta_5'' \\ -\theta_6'' \end{Bmatrix} = \begin{Bmatrix} 434.1 \\ 0 \\ 0 \\ \hdashline 554.9 \\ 544.2 \\ -465.6 \\ -465.6 \end{Bmatrix} \tag{78}$$

Solving for the displacements at the DOFs and plastic rotations in Eq. 78 gives

$$x_1 = 0.1000\,\text{m}, \quad x_2 = -0.01979\,\text{rad}, \quad x_3 = -0.01968\,\text{rad}$$

Layout: T1 Standard | Book ID: 330342_1_En | Book ISBN: 978-3-319-47796-1
Chapter No.: 6 | Date: 30-9-2016 Time: 7:37 pm | Page: 27/47

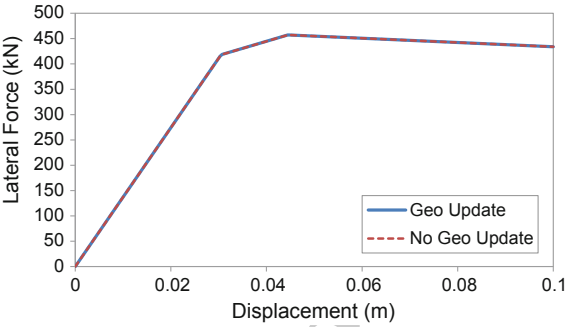

Fig. 7 Comparison of pushover curves with and without updates to geometric nonlinearity

$$\theta_1'' = 0.01715\,\text{rad}, \quad \theta_3'' = 0.01735\,\text{rad}, \quad \theta_5'' = -0.01305\,\text{rad}, \quad \theta_6'' = -0.01294\,\text{rad} \tag{79}$$

Then substituting the results in Eq. 79 back into the last six equations of Eq. 57 gives the moments

$$\begin{Bmatrix} M_1 \\ M_2 \\ M_3 \\ M_4 \\ M_5 \\ M_6 \end{Bmatrix} = \left[\begin{array}{ccc:ccc} 24085 & 34469 & 0 & 68307 & 0 & 0 & 0 \\ 24085 & 68307 & 0 & 34469 & 0 & 0 & 0 \\ 24054 & 0 & 34513 & 0 & 68132 & 0 & 0 \\ 24054 & 0 & 68132 & 0 & 34513 & 0 & 0 \\ 0 & 46034 & 23017 & 0 & 0 & 46034 & 23017 \\ 0 & 23017 & 46034 & 0 & 0 & 23017 & 46034 \end{array}\right] \begin{Bmatrix} 0.1000 \\ -0.01979 \\ -0.01968 \\ -0.01715 \\ -0.01735 \\ 0.01305 \\ 0.01294 \end{Bmatrix} = \begin{Bmatrix} 554.9 \\ 465.6 \\ 544.2 \\ 465.6 \\ -465.6 \\ -465.6 \end{Bmatrix} \tag{80}$$

and the column axial forces remain as

$$P_1 = P + (M_5 + M_6)/L_b = 890 + (-465.6 - 465.6)/6.10 = 737\,\text{kN} \tag{81a}$$

$$P_2 = P - (M_5 + M_6)/L_b = 890 - (-465.6 - 465.6)/6.10 = 1042\,\text{kN} \tag{81b}$$

Finally, the pushover curve can be plotted as shown in Fig. 7 for the case where geometric nonlinearity are updated due to the change in axial forces in the columns.

4.5 Implementation of the Analysis Procedure with no Update to Geometric Nonlinearity

As shown in Eqs. 60, 65, 70, 74, and 78, it is observed that the first entry to the stiffness matrices remain at 22,145 kN/m even when there are changes to the column axial forces. This suggests that a reduction in stiffness due to an increase in

axial force in Column 2 is offset by an increase in stiffness due to a reduction in axial force in Column 1, as presented in the stiffness matrix in Eq. 56a. Therefore, it may be interesting to investigate the differences in response when geometric nonlinearity is updated at every step of the analysis or not.

Now consider the case where geometric nonlinearity is not updated when there is a change in the column axial forces. This is achieved by using constant stiffness matrices $\mathbf{K}$, $\mathbf{K}'$, and $\mathbf{K}''$ in Eq. 57 that are computed based on the initial column axial forces throughout the analysis. By using the same one-story frame as shown in Fig. 6 with column axial loads of $P_1 = P_2 = 890$ kN, Eq. 57 becomes

$$\left[\begin{array}{ccc:ccccc:cc} 22145 & 24069 & 24069 & 24069 & 24069 & 24069 & 24069 & 0 & 0 & x_1 \\ 24069 & 114253 & 23017 & 34491 & 68219 & 0 & 0 & 46034 & 23017 & x_2 \\ 24069 & 23017 & 114253 & 0 & 0 & 34491 & 68219 & 23017 & 46034 & x_3 \\ \hdashline 24069 & 34491 & 0 & 68219 & 34491 & 0 & 0 & 0 & 0 & -\theta_1'' \\ 24069 & 68219 & 0 & 34491 & 68219 & 0 & 0 & 0 & 0 & -\theta_2'' \\ 24069 & 0 & 34491 & 0 & 0 & 68219 & 34491 & 0 & 0 & -\theta_3'' \\ 24069 & 0 & 68219 & 0 & 0 & 34491 & 68219 & 0 & 0 & -\theta_4'' \\ 0 & 46034 & 23017 & 0 & 0 & 0 & 0 & 46034 & 23017 & -\theta_5'' \\ 0 & 23017 & 46034 & 0 & 0 & 0 & 0 & 23017 & 46034 & -\theta_6'' \end{array}\right] = \left\{\begin{array}{c} F_o \\ 0 \\ 0 \\ \hdashline M_1 \\ M_2 \\ M_3 \\ M_4 \\ M_5 \\ M_6 \end{array}\right\} \tag{82}$$

Step N1: The same calculation in Step U1 above can be applied to this step, where $F_o = 414.8$ kN and $x_1 = 0.0303$ m. The moment M_3 reaches its moment capacity of 545.5 kN-m and the axial forces in the columns are $P_1 = 769$ kN and $P_2 = 1010$ kN.

Step N2: The analysis continues with PHL #3 yielded, i.e., $\theta_1'' = \theta_2'' = \theta_4'' = \theta_5'' = \theta_6'' = 0$. The lateral force is applied up to $F_o = 418.7$ kN. Rows 1, 2, 3, and 6 are extracted from Eq. 82:

$$\left[\begin{array}{ccc:c} 22145 & 24069 & 24069 & 24069 \\ 24069 & 114253 & 23017 & 0 \\ 24069 & 23017 & 114253 & 34491 \\ \hdashline 24069 & 0 & 34491 & 68219 \end{array}\right] \left\{\begin{array}{c} x_1 \\ x_2 \\ x_3 \\ \hdashline -\theta_3'' \end{array}\right\} = \left\{\begin{array}{c} 418.7 \\ 0 \\ 0 \\ \hdashline 545.5 \end{array}\right\} \tag{83}$$

Solving for the displacements at the DOFs and plastic rotations in Eq. 83 gives

$$x_1 = 0.0308\,\text{m}, \quad x_2 = -0.00540\,\text{rad}, \quad x_3 = -0.00534\,\text{rad}, \quad \theta_3'' = 0.00015\,\text{rad} \tag{84}$$

Then substituting the results in Eq. 84 back into the last six equations of Eq. 82 gives the moments

$$\begin{Bmatrix} M_1 \\ M_2 \\ M_3 \\ M_4 \\ M_5 \\ M_6 \end{Bmatrix} = \left[\begin{array}{cccc:c} 24069 & 34491 & 0 & 0 & \\ 24069 & 68219 & 0 & 0 & \\ 24069 & 0 & 34491 & 68219 & \\ 24069 & 0 & 68219 & 34491 & \\ 0 & 46034 & 23017 & 0 & \\ 0 & 23017 & 46034 & 0 & \end{array}\right] \left\{\begin{array}{c} 0.0308 \\ -0.00540 \\ -0.00534 \\ \hdashline -0.00015 \end{array}\right\} = \begin{Bmatrix} 554.0 \\ 371.7 \\ 545.5 \\ 370.4 \\ -371.7 \\ -370.4 \end{Bmatrix} \tag{85}$$

and the column axial forces are updated as

$$P_1 = P + (M_5 + M_6)/L_b = 890 + (-371.7 - 370.4)/6.10 = 768\,\text{kN} \tag{86a}$$

$$P_2 = P - (M_5 + M_6)/L_b = 890 - (-371.7 - 370.4)/6.10 = 1011\,\text{kN} \tag{86b}$$

Then using Eq. 59a to check for yielding at PHLs #1 and #3 gives

$$\text{PHL } \#1: \ (768/3843)^2 + (554.0/565.4)^2 = 1.000 \tag{87a}$$

$$\text{PHL } \#3: \ (1011/3843)^2 + (545.5/565.4)^2 = 1.000 \tag{87b}$$

which indicates that PHL #1 reaches its capacity and PHL #3 continues yielding at this step.

Step N3: The analysis continues with PHLs #1 and #3 yielded, i.e., $\theta_2'' = \theta_4'' = \theta_5'' = \theta_6'' = 0$. The lateral force is applied up to $F_o = 457.0$ kN. Rows 1, 2, 3, 4, and 6 are extracted from Eq. 82:

$$\left[\begin{array}{ccccc:cc} 22145 & 24069 & 24069 & 24069 & 24069 & & \\ 24069 & 114253 & 23017 & 34491 & 0 & & \\ 24069 & 23017 & 114253 & 0 & 34491 & & \\ \hdashline 24069 & 34491 & 0 & 68219 & 0 & & \\ 24069 & 0 & 34491 & 0 & 68219 & & \end{array}\right] \left\{\begin{array}{c} x_1 \\ x_2 \\ x_3 \\ \hdashline -\theta_1'' \\ -\theta_3'' \end{array}\right\} = \left\{\begin{array}{c} 457.0 \\ 0 \\ 0 \\ \hdashline 554.0 \\ 545.5 \end{array}\right\} \tag{88}$$

Solving for the displacements at the DOFs and plastic rotations in Eq. 88 gives

$$x_1 = 0.0445\,\text{m}, \quad x_2 = -0.00676\,\text{rad}, \quad x_3 = -0.0670\,\text{rad}$$

$$\theta_1'' = 0.00415\,\text{rad}, \quad \theta_3'' = 0.00430\,\text{rad} \tag{89}$$

Layout: T1 Standard | Book ID: 330342_1_En | Book ISBN: 978-3-319-47796-1
Chapter No.: 6 | Date: 30-9-2016 | Time: 7:37 pm | Page: 30/47

Then substituting the results in Eq. 89 back into the last six equations of Eq. 82 gives the moments

$$\begin{Bmatrix} M_1 \\ M_2 \\ M_3 \\ M_4 \\ M_5 \\ M_6 \end{Bmatrix} = \left[\begin{array}{ccc:cc:c} 24069 & 34491 & 0 & 68219 & 0 & \\ 24069 & 68219 & 0 & 34491 & 0 & \\ 24069 & 0 & 34491 & 0 & 68219 & \\ 24069 & 0 & 68219 & 0 & 34491 & \\ 0 & 46034 & 23017 & 0 & 0 & \\ 0 & 23017 & 46034 & 0 & 0 & \end{array}\right] \left\{\begin{array}{c} 0.0445 \\ -0.00676 \\ -0.00670 \\ \hdashline -0.00415 \\ -0.00430 \end{array}\right\} = \begin{Bmatrix} 553.9 \\ 465.6 \\ 545.4 \\ 464.3 \\ -465.6 \\ -464.3 \end{Bmatrix} \tag{90}$$

At this point, the moment at PHL #5 reaches its capacity of $f_Y Z_b = 465.6$ kN-m, and the column axial forces are updated as

$$P_1 = P + (M_5 + M_6)/L_b = 890 + (-465.6 - 464.3)/6.10 = 737\,\text{kN} \tag{91a}$$

$$P_2 = P - (M_5 + M_6)/L_b = 890 - (-465.6 - 464.3)/6.10 = 1042\,\text{kN} \tag{91b}$$

Step N4: The analysis continues with PHLs #1, #3, and #5 yielded, i.e., $\theta_2'' = \theta_4'' = \theta_6'' = 0$. The lateral force is applied up to $F_o = 457.1$ kN. Rows 1, 2, 3, 4, 6, and 8 are extracted from Eq. 82:

$$\left[\begin{array}{ccc:ccc} 22145 & 24069 & 24069 & 24069 & 24069 & 0 \\ 24069 & 114253 & 23017 & 34491 & 0 & 46034 \\ 24069 & 23017 & 114253 & 0 & 34491 & 23017 \\ \hdashline 24069 & 34491 & 0 & 68219 & 0 & 0 \\ 24069 & 0 & 34491 & 0 & 68219 & 0 \\ 0 & 46034 & 23017 & 0 & 0 & 46034 \end{array}\right] \left\{\begin{array}{c} x_1 \\ x_2 \\ x_3 \\ \hdashline -\theta_1'' \\ -\theta_3'' \\ -\theta_5'' \end{array}\right\} = \left\{\begin{array}{c} 457.1 \\ 0 \\ 0 \\ \hdashline 553.9 \\ 545.4 \\ -465.6 \end{array}\right\} \tag{92}$$

Solving for the displacements at the DOFs and plastic rotations in Eq. 92 gives

$$x_1 = 0.0448\,\text{m}, \quad x_2 = -0.00685\,\text{rad}, \quad x_3 = -0.00674\,\text{rad}$$

$$\theta_1'' = 0.00420\,\text{rad}, \quad \theta_3'' = 0.00442\,\text{rad}, \quad \theta_5'' = -0.00011\,\text{rad} \tag{93}$$

Then substituting the results in Eq. 93 back into the last six equations of Eq. 82 gives the moments

$$\begin{Bmatrix} M_1 \\ M_2 \\ M_3 \\ M_4 \\ M_5 \\ M_6 \end{Bmatrix} = \left[\begin{array}{ccc:ccc} 24069 & 34491 & 0 & 68219 & 0 & 0 \\ 24069 & 68219 & 0 & 34491 & 0 & 0 \\ 24069 & 0 & 34491 & 0 & 68219 & 0 \\ 24069 & 0 & 68219 & 0 & 34491 & 0 \\ 0 & 46034 & 23017 & 0 & 0 & 46034 \\ 0 & 23017 & 46034 & 0 & 0 & 23017 \end{array}\right] \left\{\begin{array}{c} 0.0448 \\ -0.00685 \\ -0.00674 \\ \hdashline -0.00420 \\ -0.00442 \\ 0.00011 \end{array}\right\} = \begin{Bmatrix} 554.9 \\ 465.6 \\ 544.2 \\ 465.6 \\ -465.6 \\ -465.6 \end{Bmatrix} \tag{94}$$

Layout: T1 Standard | Book ID: 330342_1_En | Book ISBN: 978-3-319-47796-1
Chapter No.: 6 | Date: 30-9-2016 | Time: 7:37 pm | Page: 31/47

At this point, the moment at PHL #6 reaches its capacity of $f_Y Z_b = 465.6$ kN-m, and the column axial forces are updated as

$$P_1 = P + (M_5 + M_6)/L_b = 890 + (-465.6 - 465.6)/6.10 = 737\,\text{kN} \quad (95a)$$

$$P_2 = P - (M_5 + M_6)/L_b = 890 - (-465.6 - 465.6)/6.10 = 1042\,\text{kN} \quad (95b)$$

Step N5: Now that a mechanism has developed with the formation of plastic hinges at PHLs #1, #3, #5, and #6, the frame will continue to deflect without any additional load. Let the analysis continue with PHLs #1, #3, #5, and #6 yielded, i.e., $\theta_2'' = \theta_4'' = 0$. By using any applied lateral force less than $F_o = 457.1$ kN (from Step N4), say $F_o = 434.1$ kN, Rows 1, 2, 3, 4, 6, 8, and 9 are extracted from Eq. 82:

$$\left[\begin{array}{ccc:ccc:c} 22145 & 24069 & 24069 & 24069 & 24069 & 0 & 0 \\ 24069 & 114253 & 23017 & 34491 & 0 & 46034 & 23017 \\ 24069 & 23017 & 114253 & 0 & 34491 & 23017 & 46034 \\ \hdashline 24069 & 34491 & 0 & 68219 & 0 & 0 & 0 \\ 24069 & 0 & 34491 & 0 & 68219 & 0 & 0 \\ 0 & 46034 & 23017 & 0 & 0 & 46034 & 23017 \\ 0 & 23017 & 46034 & 0 & 0 & 23017 & 46034 \end{array}\right] \left\{\begin{array}{c} x_1 \\ x_2 \\ x_3 \\ \hdashline -\theta_1'' \\ -\theta_3'' \\ -\theta_5'' \\ -\theta_6'' \end{array}\right\} = \left\{\begin{array}{c} 434.1 \\ 0 \\ 0 \\ \hdashline 554.9 \\ 544.2 \\ -465.6 \\ -465.6 \end{array}\right\} \quad (96)$$

Solving for the displacements at the DOFs and plastic rotations in Eq. 96 gives

$$x_1 = 0.1000\,\text{m}, \quad x_2 = -0.01979\,\text{rad}, \quad x_3 = -0.01968\,\text{rad}$$

$$\theta_1'' = 0.01714\,\text{rad}, \quad \theta_3'' = 0.01735\,\text{rad}, \quad \theta_5'' = -0.01305\,\text{rad}, \quad \theta_6'' = -0.01294\,\text{rad} \quad (97)$$

Then substituting the results in Eq. 97 back into the last six equations of Eq. 57 gives the moments

Table 1 Comparison of plastic rotations with and without updates to geometric nonlinearity

Step	Plastic rotation (rad) with geo update				Plastic rotation (rad) with no update			
	PHL #1	PHL #3	PHL #5	PHL #6	PHL #1	PHL #3	PHL #5	PHL #6
1	0	0	0	0	0	0	0	0
2	0	0.00014	0	0	0	0.00015	0	0
3	0.00415	0.00429	0	0	0.00415	0.00430	0	0
4	0.00421	0.00441	0.00011	0	0.00420	0.00442	0.00011	0
5	0.01715	0.01735	0.01305	0.01294	0.01714	0.01735	0.01305	0.01294

Layout: T1 Standard | Book ID: 330342_1_En | Book ISBN: 978-3-319-47796-1
Chapter No.: 6 | Date: 30-9-2016 Time: 7:37 pm | Page: 32/47

$$\begin{Bmatrix} M_1 \\ M_2 \\ M_3 \\ M_4 \\ M_5 \\ M_6 \end{Bmatrix} = \left[\begin{array}{ccc:ccc:c} 24069 & 34491 & 0 & 68219 & 0 & 0 & 0 \\ 24069 & 68219 & 0 & 34491 & 0 & 0 & 0 \\ 24069 & 0 & 34491 & 0 & 68219 & 0 & 0 \\ 24069 & 0 & 68219 & 0 & 34491 & 0 & 0 \\ 0 & 46034 & 23017 & 0 & 0 & 46034 & 23017 \\ 0 & 23017 & 46034 & 0 & 0 & 23017 & 46034 \end{array}\right] \left\{\begin{array}{c} 0.1000 \\ -0.01979 \\ -0.01968 \\ -0.01714 \\ -0.01735 \\ 0.01305 \\ 0.01294 \end{array}\right\} = \begin{Bmatrix} 554.9 \\ 465.6 \\ 544.2 \\ 465.6 \\ -465.6 \\ -465.6 \end{Bmatrix} \quad (98)$$

and the column axial forces remain as

$$P_1 = P + (M_5 + M_6)/L_b = 890 + (-465.6 - 465.6)/6.10 = 737\,\text{kN} \quad (99a)$$

$$P_2 = P - (M_5 + M_6)/L_b = 890 - (-465.6 - 465.6)/6.10 = 1042\,\text{kN} \quad (99b)$$

The pushover curve is plotted as shown in Fig. 7 for the case where the update of stiffness matrix due to geometric nonlinearity is ignored when axial forces in the columns change. It is observed that there is practically no difference in the "global" response between whether geometric nonlinearity due to changes in axial forces in the columns for the one-story frame is updated or not. The reason is that while the induced lateral displacement imposes overturning moment on the entire framed structure, global equilibrium requires that there will be an increase in column compression on one side of the frame and an equal amount of reduction in column compression on the opposite side of the frame in order to resist the imposed overturning moment. While an increase in column compression on one side of the frame reduces the lateral stiffness of these columns, a reduction in column compression on the opposite side of the frame increases the lateral stiffness of those columns by a similar amount. The end result is that the net change in total lateral stiffness of the entire frame becomes negligible, and this can be observed when the stiffness matrix in Eq. 65 (**Step U2**) is compared with that in Eq. 83 (**Step N2**). Similar observations can also be made when the stiffness matrix in Eq. 70 (**Step U3**) is compared with that in Eq. 88 (**Step N3**). Therefore, an assumption to keep the geometrically nonlinear stiffness matrices unchanged throughout the analysis even as loading increases is reasonable, and this is consistent with the recommendation by Wilson [15] that P–Δ analysis method "does not require iteration because the total axial force at a story level is equal to the weight of the building above that level and does not change during the application of lateral loads". This observation is important in nonlinear dynamic analysis of moment-resisting frames because significant computational effort can be reduced with reasonable accuracy by using the approximation of constant geometrically nonlinear stiffness matrices. AQ1

Table 1 summarizes the plastic rotation results obtained in the above analysis procedure. It can be seen that the differences in plastic rotations between whether geometric nonlinearity is updated or not updated is negligible. This suggests that there is practically no difference in the "local" response between whether geometric nonlinearity due to changes in axial forces in the columns for the one-story frame is updated or not, even at a drift ratio of 1.6 % (i.e., $0.10/6.10 = 0.0164$).

Layout: T1 Standard | Book ID: 330342_1_En | Book ISBN: 978-3-319-47796-1
Chapter No.: 6 | Date: 30-9-2016 Time: 7:37 pm | Page: 33/47

5 Nonlinear Dynamic Analysis of Framed Structures

In the previous section, the global stiffness matrices incorporating both geometric and material nonlinearities are used to determine the static behavior and plastic rotation response of structures. In this section, the analysis procedure with plastic rotation calculations is extended to nonlinear dynamic analysis. For an n-DOF system subjected to earthquake ground motions, the equation of motion can be written as

$$\mathbf{m}\ddot{\mathbf{x}}(t) + \mathbf{c}\dot{\mathbf{x}}(t) + \mathbf{K}(t)\mathbf{x}'(t) = -\mathbf{m}\ddot{\mathbf{g}}(t) - \mathbf{F}_a(t) \tag{100}$$

where $\mathbf{m}$ is the $n \times n$ mass matrix, $\mathbf{c}$ is the $n \times n$ damping matrix, $\dot{\mathbf{x}}(t)$ is the $n \times 1$ velocity vector, $\ddot{\mathbf{x}}(t)$ is the $n \times 1$ acceleration vector, $\mathbf{K}(t)$ is the time-varying $n \times n$ stiffness matrix derived in Eq. 28a while subjected to time-varying column axial compressive forces, $\ddot{\mathbf{g}}(t)$ is the $n \times 1$ earthquake ground acceleration vector corresponding to the effect of ground motion at each DOF, and $\mathbf{F}_a(t)$ is the $n \times 1$ vector of additional forces imposed on the frame due to geometric nonlinearity of all the gravity columns in the structure (mainly the P−Δ effect). This nonlinearity can often be modeled using a leaning column (or sometimes called a P−Δ column) in a two-dimensional analysis but may require more detailed modeling of all gravity columns in a three-dimensional analysis that may affect the response due to torsional irregularity of the structure. In a two-dimensional analysis, the relationship between this lateral force $\mathbf{F}_a(t)$ and the lateral displacement can be written as:

$$\mathbf{F}_a(t) = \mathbf{K}_a\mathbf{x}(t) \tag{101}$$

where $\mathbf{K}_a$ is an $n \times n$ stiffness matrix that is a function of the gravity loads on the leaning column and the corresponding story height, but it is not a function of time. For two-dimensional frames with horizontal degrees of freedom only, this $\mathbf{K}_a$ matrix often takes the form:

$$\mathbf{K}_a = \begin{bmatrix} -Q_1/h_1 - Q_2/h_2 & Q_2/h_2 & 0 & \cdots & 0 \\ Q_2/h_2 & -Q_2/h_2 - Q_3/h_3 & \ddots & \ddots & \vdots \\ 0 & \ddots & \ddots & Q_{n-1}/h_{n-1} & 0 \\ \vdots & \ddots & Q_{n-1}/h_{n-1} & -Q_{n-1}/h_{n-1} - Q_n/h_n & Q_n/h_n \\ 0 & \cdots & 0 & Q_n/h_n & -Q_n/h_n \end{bmatrix} \tag{102}$$

where Q_i is the total axial force due to gravity on the leaning column of the ith floor, and h_i is the story height of the ith floor.

While the lateral force $\mathbf{F}_a(t)$ takes care of the nonlinear geometric effects from all the gravity columns in the structure, the stiffness matrix $\mathbf{K}(t)$ in Eq. 100 considers both large P−Δ and small P−δ effects of geometric nonlinearity on the

Layout: T1 Standard | Book ID: 330342_1_En | Book ISBN: 978-3-319-47796-1
Chapter No.: 6 | Date: 30-9-2016 Time: 7:37 pm | Page: 34/47

moment-resisting frame itself. Let this time-dependent global stiffness matrix $\mathbf{K}(t)$ be represented in the form:

$$\mathbf{K}(t) = \mathbf{K}_L + \mathbf{K}_G(t) \tag{103}$$

where $\mathbf{K}_L$ denotes the linearized elastic stiffness of the frame due to the gravity loads only, and $\mathbf{K}_G(t)$ denotes the change in stiffness due to the change in axial load on members during the dynamic loading. Since the $\mathbf{K}_L$ matrix is computed by using the gravity loads on the columns (which means $\mathbf{K}_L = \mathbf{K}(t_0) = \mathbf{K}(0)$, i.e., the stiffness matrix computed at time step 0) only, it is not a function of time and therefore remains as a constant throughout the dynamic analysis.

The state space method of dynamic analysis uses explicit formulation, which is a desirable method when nonlinearity is involved. Therefore it is used here in the derivation of the analysis procedure. However, it requires that the mass matrix $\mathbf{m}$ in Eq. 100 be invertible. In many practical structural analysis problems, masses at certain DOFs are intentionally set to zero in order to reduce the number of DOFs in the structural model. When the mass is zero at certain DOFs, such as those DOFs related to the vertical translation and joint rotations, the mass matrix in Eq. 100 will become singular and therefore the state space method cannot be readily employed. To overcome this problem with non-invertible (or singular) mass matrix, static condensation is first applied in order to eliminate those DOFs with zero mass or mass moment of inertia before solving the dynamic problem.

5.1 Static Condensation for Nonlinear Dynamic Analysis

Consider a moment-resisting frame with n DOFs and m PHLs as presented in Eq. 100, the equation of motion can be partitioned in the matrix form as

$$\left[\begin{array}{c|c} \mathbf{m}_{dd} & \mathbf{0} \\ \hline \mathbf{0} & \mathbf{0} \end{array}\right]\left\{\begin{array}{c} \ddot{\mathbf{x}}_d(t) \\ \hline \ddot{\mathbf{x}}_r(t) \end{array}\right\} + \left[\begin{array}{c|c} \mathbf{c}_{dd} & \mathbf{0} \\ \hline \mathbf{0} & \mathbf{0} \end{array}\right]\left\{\begin{array}{c} \dot{\mathbf{x}}_d(t) \\ \hline \dot{\mathbf{x}}_r(t) \end{array}\right\} + \left[\begin{array}{c|c} \mathbf{K}_{dd}(t) & \mathbf{K}_{dr}(t) \\ \hline \mathbf{K}_{rd}(t) & \mathbf{K}_{rr}(t) \end{array}\right]\left\{\begin{array}{c} \mathbf{x}'_d(t) \\ \hline \mathbf{x}'_r(t) \end{array}\right\} = -\left[\begin{array}{c|c} \mathbf{m}_{dd} & \mathbf{0} \\ \hline \mathbf{0} & \mathbf{0} \end{array}\right]\left\{\begin{array}{c} \ddot{\mathbf{g}}_d(t) \\ \hline \mathbf{0} \end{array}\right\} - \left\{\begin{array}{c} \mathbf{F}_a(t) \\ \hline \mathbf{0} \end{array}\right\} \tag{104}$$

where $\mathbf{m}_{dd}$ is the mass matrix associated with DOFs with mass only, $\mathbf{c}_{dd}$ is the damping matrix associated with DOFs with mass only, and $\mathbf{K}_{dd}(t)$, $\mathbf{K}_{dr}(t)$, $\mathbf{K}_{rd}(t)$, and $\mathbf{K}_{rr}(t)$ are the stiffness submatrices partitioned according to the DOFs with mass and those with zero mass. The vector $\mathbf{x}'(t)$ is the elastic displacement response, $\dot{\mathbf{x}}(t)$ is the velocity response, $\ddot{\mathbf{x}}(t)$ is the acceleration response, $\mathbf{F}_a(t)$ is the $d \times 1$ vector of additional forces imposed on the translational DOFs due to geometric nonlinearity of gravity columns, and the earthquake ground acceleration vector $\ddot{\mathbf{g}}_d(t)$ corresponds to the effect of a ground motion on each DOF associated with nonzero mass. The subscript d denotes the number of degrees of freedom that have nonzero mass, and subscript r denotes the number of degrees of freedom that

Layout: T1 Standard | Book ID: 330342_1_En | Book ISBN: 978-3-319-47796-1
Chapter No.: 6 | Date: 30-9-2016 Time: 7:37 pm | Page: 35/47

have zero mass and zero moment of inertia. This gives $n = d + r$ in an n-DOF system.

Equations 52 and 42 related to material nonlinearity can similarly be partitioned as follows:

$$\mathbf{M}(t) + \mathbf{K}''(t)\boldsymbol{\Theta}''(t) = \left[\mathbf{K}'_d(t)^T \;\vdots\; \mathbf{K}'_r(t)^T\right]\left\{\begin{matrix}\mathbf{x}_d(t)\\ \hdashline \mathbf{x}_r(t)\end{matrix}\right\} \tag{105}$$

$$\left\{\begin{matrix}\mathbf{x}''_d(t)\\ \hdashline \mathbf{x}''_r(t)\end{matrix}\right\} = \left[\begin{array}{c:c}\mathbf{K}_{dd}(t) & \mathbf{K}_{dr}(t)\\ \hdashline \mathbf{K}_{rd}(t) & \mathbf{K}_{rr}(t)\end{array}\right]^{-1}\left[\begin{matrix}\mathbf{K}'_d(t)\\ \hdashline \mathbf{K}'_r(t)\end{matrix}\right]\boldsymbol{\Theta}''(t) \tag{106}$$

where

$$\mathbf{K}'(t) = \left[\begin{matrix}\mathbf{K}'_d(t)\\ \hdashline \mathbf{K}'_r(t)\end{matrix}\right] \quad , \quad \mathbf{x}''(t) = \left\{\begin{matrix}\mathbf{x}''_d(t)\\ \hdashline \mathbf{x}''_r(t)\end{matrix}\right\} \quad , \quad \left\{\begin{matrix}\mathbf{x}_d(t)\\ \hdashline \mathbf{x}_r(t)\end{matrix}\right\} = \left\{\begin{matrix}\mathbf{x}'_d(t)\\ \hdashline \mathbf{x}'_r(t)\end{matrix}\right\} + \left\{\begin{matrix}\mathbf{x}''_d(t)\\ \hdashline \mathbf{x}''_r(t)\end{matrix}\right\} \tag{107}$$

Static condensation is now performed on Eq. 104. The second equation of Eq. 104 is extracted and written in the long form as

$$\mathbf{K}_{rd}(t)\mathbf{x}'_d(t) + \mathbf{K}_{rr}(t)\mathbf{x}'_r(t) = \mathbf{0} \tag{108}$$

Solving for $\mathbf{x}'_r(t)$ in Eq. 108 gives

$$\mathbf{x}'_r(t) = -\mathbf{K}_{rr}^{-1}(t)\mathbf{K}_{rd}(t)\mathbf{x}'_d(t) \tag{109}$$

Now substituting Eq. 109 back into the first equation of Eq. 104 gives

$$\begin{aligned}&\mathbf{m}_{dd}\ddot{\mathbf{x}}_d(t) + \mathbf{c}_{dd}\dot{\mathbf{x}}_d(t) + \mathbf{K}_{dd}(t)\mathbf{x}'_d(t) - \mathbf{K}_{dr}(t)\mathbf{K}_{rr}^{-1}(t)\mathbf{K}_{rd}(t)\mathbf{x}'_d(t)\\ &\quad = -\mathbf{m}_{dd}\ddot{\mathbf{g}}_d(t) - \mathbf{F}_a(t)\end{aligned} \tag{110}$$

Define

$$\overline{\mathbf{K}}(t) = \mathbf{K}_{dd}(t) - \mathbf{K}_{dr}(t)\mathbf{K}_{rr}^{-1}(t)\mathbf{K}_{rd}(t) \tag{111}$$

Then Eq. 110 becomes

$$\mathbf{m}_{dd}\ddot{\mathbf{x}}_d(t) + \mathbf{c}_{dd}\dot{\mathbf{x}}_d(t) + \overline{\mathbf{K}}(t)\mathbf{x}'_d(t) = -\mathbf{m}_{dd}\ddot{\mathbf{g}}_d(t) - \mathbf{F}_a(t) \tag{112}$$

which represents the equation of motion in the statically condensed form.

Since Eqs. 105 and 106 contain both DOFs with mass (i.e., $\mathbf{x}_d(t)$ and $\mathbf{x}''_d(t)$) and DOFs without mass (i.e., $\mathbf{x}_r(t)$ and $\mathbf{x}''_r(t)$), static condensation must also be applied to these two equations to reduce the DOFs to those with mass only. Considering Eq. 106 and pre-multiplying both sides of this equation by the stiffness matrix $\mathbf{K}(t)$ gives

$$\left[\begin{array}{c:c}\mathbf{K}_{dd}(t) & \mathbf{K}_{dr}(t)\\ \hdashline \mathbf{K}_{rd}(t) & \mathbf{K}_{rr}(t)\end{array}\right]\left\{\begin{matrix}\mathbf{x}''_d(t)\\ \hdashline \mathbf{x}''_r(t)\end{matrix}\right\} = \left[\begin{matrix}\mathbf{K}'_d\\ \hdashline \mathbf{K}'_r\end{matrix}\right]\boldsymbol{\Theta}''(t) \tag{113}$$

Extracting the second equation of Eq. 113 and solving for $\mathbf{x}''_r(t)$ gives

$$\mathbf{x}_r''(t) = -\mathbf{K}_{rr}^{-1}(t)\mathbf{K}_{rd}(t)\mathbf{x}_d''(t) + \mathbf{K}_{rr}^{-1}(t)\mathbf{K}_r'(t)\boldsymbol{\Theta}''(t) \tag{114}$$

Now substituting Eq. 114 back into the first equation of Eq. 113 gives

$$\mathbf{K}_{dd}(t)\mathbf{x}_d''(t) + \mathbf{K}_{dr}(t)\left[-\mathbf{K}_{rr}^{-1}(t)\mathbf{K}_{rd}(t)\mathbf{x}_d''(t) + \mathbf{K}_{rr}^{-1}(t)\mathbf{K}_r'(t)\boldsymbol{\Theta}''(t)\right] = \mathbf{K}_d'\boldsymbol{\Theta}''(t) \tag{115}$$

and rearranging the terms gives

$$\left[\mathbf{K}_{dd}(t) - \mathbf{K}_{dr}(t)\mathbf{K}_{rr}^{-1}(t)\mathbf{K}_{rd}(t)\right]\mathbf{x}_d''(t) = \left[\mathbf{K}_d'(t) - \mathbf{K}_{dr}(t)\mathbf{K}_{rr}^{-1}(t)\mathbf{K}_r'(t)\right]\boldsymbol{\Theta}''(t) \tag{116}$$

Define

$$\overline{\mathbf{K}}'(t) = \mathbf{K}_d'(t) - \mathbf{K}_{dr}(t)\mathbf{K}_{rr}^{-1}(t)\mathbf{K}_r'(t) \tag{117}$$

Substituting Eqs. 111 and 117 into Eq. 116 gives

$$\overline{\mathbf{K}}(t)\mathbf{x}_d''(t) = \overline{\mathbf{K}}'(t)\boldsymbol{\Theta}''(t) \tag{118}$$

Finally, pre-multiplying both sides of Eq. 118 by the inverse of the condensed global stiffness matrix in Eq. 111 (i.e., $\overline{\mathbf{K}}(t)^{-1}$) gives

$$\mathbf{x}_d''(t) = \overline{\mathbf{K}}(t)^{-1}\overline{\mathbf{K}}'(t)\boldsymbol{\Theta}''(t) \tag{119}$$

which represents the condensed form of Eq. 106.

Finally, considering Eq. 105 and expanding the right hand side this equation gives

$$\mathbf{M}(t) + \mathbf{K}''(t)\boldsymbol{\Theta}''(t) = \mathbf{K}_d'(t)^T\mathbf{x}_d(t) + \mathbf{K}_r'(t)^T\mathbf{x}_r(t) \tag{120}$$

The term $\mathbf{x}_r(t)$ in Eq. 120 must be first calculated. Since $\mathbf{x}_r(t) = \mathbf{x}_r'(t) + \mathbf{x}_r''(t)$ according to Eq. 107, substituting Eqs. 109 and 114 into this equation gives

$$\begin{aligned}\mathbf{x}_r(t) &= \mathbf{x}_r'(t) + \mathbf{x}_r''(t) \\ &= -\mathbf{K}_{rr}^{-1}(t)\mathbf{K}_{rd}(t)\mathbf{x}_d'(t) - \mathbf{K}_{rr}^{-1}(t)\mathbf{K}_{rd}(t)\mathbf{x}_d''(t) + \mathbf{K}_{rr}^{-1}(t)\mathbf{K}_r'(t)\boldsymbol{\Theta}''(t)\end{aligned} \tag{121}$$

Also, since $\mathbf{x}_d'(t) + \mathbf{x}_d''(t) = \mathbf{x}_d(t)$ according to Eq. 107, substituting this equation in Eq. 121 gives

$$\mathbf{x}_r(t) = -\mathbf{K}_{rr}^{-1}(t)\mathbf{K}_{rd}(t)\mathbf{x}_d(t) + \mathbf{K}_{rr}^{-1}(t)\mathbf{K}_r'(t)\boldsymbol{\Theta}''(t) \tag{122}$$

Now substituting Eq. 122 into Eq. 120 and rearranging the terms gives

$$\mathbf{M}(t) + \left[\mathbf{K}''(t) - \mathbf{K}'_r(t)^T \mathbf{K}_{rr}^{-1}(t)\mathbf{K}'_r(t)\right] \boldsymbol{\Theta}''(t) = \left[\mathbf{K}'_d(t)^T - \mathbf{K}'_r(t)^T \mathbf{K}_{rr}^{-1}(t)\mathbf{K}_{rd}(t)\right] \mathbf{x}_d(t) \tag{123}$$

Define

$$\overline{\mathbf{K}}''(t) = \mathbf{K}''(t) - \mathbf{K}'_r(t)^T \mathbf{K}_{rr}^{-1}(t)\mathbf{K}'_r(t) \tag{124}$$

Substituting Eqs. 117 and 124 into Eq. 123 gives

$$\mathbf{M}(t) + \overline{\mathbf{K}}''(t)\boldsymbol{\Theta}''(t) = \overline{\mathbf{K}}'(t)^T \mathbf{x}_d(t) \tag{125}$$

which represents the condensed form of Eq. 105.

5.2 Nonlinear Dynamic Analysis Procedure

By applying static condensation to eliminate the DOFs associated with zero mass and zero mass moment of inertia (i.e., $\mathbf{x}_r(t)$), the resulting equations for nonlinear dynamic analysis are presented in Eqs. 112, 125, and 119, which are rewritten here:

$$\mathbf{m}_{dd}\ddot{\mathbf{x}}_d(t) + \mathbf{c}_{dd}\dot{\mathbf{x}}_d(t) + \overline{\mathbf{K}}(t)\mathbf{x}'_d(t) = -\mathbf{m}_{dd}\ddot{\mathbf{g}}_d(t) - \mathbf{F}_a(t) \tag{126a}$$

$$\mathbf{M}(t) + \overline{\mathbf{K}}''(t)\boldsymbol{\Theta}''(t) = \overline{\mathbf{K}}'(t)^T \mathbf{x}_d(t) \tag{126b}$$

$$\mathbf{x}''_d(t) = \overline{\mathbf{K}}(t)^{-1}\overline{\mathbf{K}}'(t)\boldsymbol{\Theta}''(t) \tag{126c}$$

where according to Eqs. 111, 117, and 124, the statically condensed global stiffness matrices are:

$$\overline{\mathbf{K}}(t) = \mathbf{K}_{dd}(t) - \mathbf{K}_{dr}(t)\mathbf{K}_{rr}^{-1}(t)\mathbf{K}_{rd}(t) \tag{127a}$$

$$\overline{\mathbf{K}}'(t) = \mathbf{K}'_d(t) - \mathbf{K}_{dr}(t)\mathbf{K}_{rr}^{-1}(t)\mathbf{K}'_r(t) \tag{127b}$$

$$\overline{\mathbf{K}}''(t) = \mathbf{K}''(t) - \mathbf{K}'_r(t)^T \mathbf{K}_{rr}^{-1}(t)\mathbf{K}'_r(t) \tag{127c}$$

and Eqs. 101 and 103 can be written in the forms:

$$\mathbf{F}_a(t) = \mathbf{K}_a \mathbf{x}_d(t), \quad \overline{\mathbf{K}}(t) = \overline{\mathbf{K}}_L + \overline{\mathbf{K}}_G(t) \tag{128}$$

where again $\mathbf{K}_a$ denotes the lateral stiffness due to the gravity columns and $\overline{\mathbf{K}}_L$ denotes the linearized elastic stiffness of the moment-resisting frame only. Solving for the elastic displacement $\mathbf{x}'_d(t)$ in Eq. 107 gives $\mathbf{x}'_d(t) = \mathbf{x}_d(t) - \mathbf{x}''_d(t)$, and substituting the result into Eq. 126a gives

$$\mathbf{m}_{dd}\ddot{\mathbf{x}}_d(t) + \mathbf{c}_{dd}\dot{\mathbf{x}}_d(t) + \overline{\mathbf{K}}(t)\mathbf{x}_d(t) = -\mathbf{m}_{dd}\ddot{\mathbf{g}}_d(t) - \mathbf{F}_a(t) + \overline{\mathbf{K}}(t)\mathbf{x}_d''(t) \tag{129}$$

Then substituting Eq. 128 into Eq. 129, the equation of motion after considering both large $P{-}\Delta$ and small $P{-}\delta$ effects of geometric nonlinearity of the entire structure becomes

$$\mathbf{m}_{dd}\ddot{\mathbf{x}}_d(t) + \mathbf{c}_{dd}\dot{\mathbf{x}}_d(t) + \overline{\mathbf{K}}_L\mathbf{x}_d(t) = -\mathbf{m}_{dd}\ddot{\mathbf{g}}_d(t) - \mathbf{K}_a\mathbf{x}_d(t) - \overline{\mathbf{K}}_G(t)\mathbf{x}_d(t) + \overline{\mathbf{K}}(t)\mathbf{x}_d''(t) \tag{130}$$

Define

$$\overline{\mathbf{K}}_e = \overline{\mathbf{K}}_L + \mathbf{K}_a \tag{131}$$

where $\overline{\mathbf{K}}_e$ represents the elastic stiffness of the entire structure (i.e., the sum of elastic stiffness of the moment-resisting frame and that of the gravity columns). Substituting Eq. 131 into Eq. 130, it follows that

$$\mathbf{m}_{dd}\ddot{\mathbf{x}}_d(t) + \mathbf{c}_{dd}\dot{\mathbf{x}}_d(t) + \overline{\mathbf{K}}_e\mathbf{x}_d(t) = -\mathbf{m}_{dd}\ddot{\mathbf{g}}_d(t) - \overline{\mathbf{K}}_G(t)\mathbf{x}_d(t) + \overline{\mathbf{K}}(t)\mathbf{x}_d''(t) \tag{132}$$

This equation of motion can now be solved using the state space method. To represent Eq. 132 in state space form, let the state vector $\mathbf{z}(t)$ be defined as

$$\mathbf{z}(t) = \begin{Bmatrix} \mathbf{x}_d(t) \\ \dot{\mathbf{x}}_d(t) \end{Bmatrix} \tag{133}$$

which is a $2d \times 1$ vector with a collection of states of the responses. It follows from Eq. 132 that

$$\begin{aligned} \dot{\mathbf{z}}(t) = \begin{Bmatrix} \dot{\mathbf{x}}_d(t) \\ \ddot{\mathbf{x}}_d(t) \end{Bmatrix} &= \begin{bmatrix} \mathbf{0} & \mathbf{I} \\ -\mathbf{m}_{dd}^{-1}\overline{\mathbf{K}}_e & -\mathbf{m}_{dd}^{-1}\mathbf{c}_{dd} \end{bmatrix} \begin{Bmatrix} \mathbf{x}_d(t) \\ \dot{\mathbf{x}}_d(t) \end{Bmatrix} \\ &+ \begin{bmatrix} \mathbf{0} \\ -\mathbf{h} \end{bmatrix} \mathbf{a}(t) + \begin{bmatrix} \mathbf{0} \\ \mathbf{m}_{dd}^{-1} \end{bmatrix} \left(\overline{\mathbf{K}}_e(t)\mathbf{x}_d''(t) - \overline{\mathbf{K}}_G(t)\mathbf{x}_d(t)\right) \end{aligned} \tag{134}$$

where $\mathbf{h}$ is a $d \times 3$ matrix that relates the directions of each DOF with the global X-, Y-, and Z-directions (i.e., a collection of 0's and 1's in all entries), and $\mathbf{a}(t)$ is the 3×1 ground acceleration vector in the three global directions of $\ddot{g}_X(t)$, $\ddot{g}_Y(t)$, and $\ddot{g}_Z(t)$. The relationship between the ground acceleration vector $\ddot{\mathbf{g}}_d(t)$ for each DOF in Eq. 132 and the three-component ground acceleration vector $\mathbf{a}(t)$ in Eq. 134 can be expressed as

$$\ddot{\mathbf{g}}_d(t) = \mathbf{h}\mathbf{a}(t) = \mathbf{h}\begin{Bmatrix} \ddot{g}_X(t) \\ \ddot{g}_Y(t) \\ \ddot{g}_Z(t) \end{Bmatrix} \tag{135}$$

Layout: T1 Standard | Book ID: 330342_1_En | Book ISBN: 978-3-319-47796-1
Chapter No.: 6 | Date: 30-9-2016 Time: 7:37 pm | Page: 39/47

To simplify Eq. 134, let

$$\mathbf{A} = \begin{bmatrix} \mathbf{0} & \mathbf{I} \\ -\mathbf{m}_{dd}^{-1}\overline{\mathbf{K}}_e & -\mathbf{m}_{dd}^{-1}\mathbf{c}_{dd} \end{bmatrix}, \quad \mathbf{H} = \begin{bmatrix} \mathbf{0} \\ -\mathbf{h} \end{bmatrix}, \quad \mathbf{B} = \begin{bmatrix} \mathbf{0} \\ -\mathbf{m}_{dd}^{-1} \end{bmatrix} \tag{136a}$$

$$\mathbf{f}_G(t) = -\overline{\mathbf{K}}_G(t)\mathbf{x}_d(t), \quad \mathbf{f}_M(t) = \overline{\mathbf{K}}(t)\mathbf{x}_d''(t) \tag{136b}$$

where $\mathbf{A}$ is the $2d \times 2d$ state transition matrix in the continuous form, $\mathbf{H}$ is the $2d \times 3$ ground motion transition matrix in the continuous form, $\mathbf{B}$ is the $2d \times d$ nonlinearity transition matrix in the continuous form, $\mathbf{f}_G(t)$ is the $d \times 1$ equivalent force vector due to geometric nonlinearity, and $\mathbf{f}_M(t)$ is the $d \times 1$ equivalent force vector due to material nonlinearity. Then Eq. 134 becomes

$$\dot{\mathbf{z}}(t) = \mathbf{A}\mathbf{z}(t) + \mathbf{H}\mathbf{a}(t) + \mathbf{B}\mathbf{f}_G(t) + \mathbf{B}\mathbf{f}_M(t) \tag{137}$$

Solving for the first-order linear differential equation in Eq. 137 gives

$$\mathbf{z}(t) = \mathbf{e}^{\mathbf{A}(t-t_o)}\,\mathbf{z}(t_o) + \mathbf{e}^{\mathbf{A}t}\int_{t_o}^{t} \mathbf{e}^{-\mathbf{A}s}[\,\mathbf{H}\mathbf{a}(s) + \mathbf{B}\mathbf{f}_G(s) + \mathbf{B}\mathbf{f}_M(s)]ds \tag{138}$$

where t_o is the time of reference when the integration begins, which is typically the time when the states are known. In a recursive analysis procedure, the known states are often taken at the current time step $\mathbf{z}(t_o)$ and the objective is to calculate the states at the next time step $\mathbf{z}(t)$. Therefore, let $t_{k+1} = t$, $t_k = t_o$, and $\Delta t = t_{k+1} - t_k$, and the subscript k denotes the kth time step, then it follows from Eq. 138 that

$$\mathbf{z}_{k+1} = \mathbf{e}^{\mathbf{A}\Delta t}\,\mathbf{z}_k + \mathbf{e}^{\mathbf{A}t_{k+1}}\int_{t_k}^{t_{k+1}} \mathbf{e}^{-\mathbf{A}s}\,[\mathbf{H}\mathbf{a}(s) + \mathbf{B}\mathbf{f}_G(s) + \mathbf{B}\mathbf{f}_M(s)]\,ds \tag{139}$$

By using the Dirac delta function approximation for the variables in the integral for the purpose of carrying out the integration, the ground acceleration vector $\mathbf{a}(s)$, equivalent geometric nonlinear force vector $\mathbf{f}_G(s)$, and equivalent material nonlinear force vector $\mathbf{f}_M(s)$ take the form:

$$\mathbf{a}(s) = \mathbf{a}_k\delta(s - t_k)\Delta t \quad , \quad t_k \le s < t_{k+1} \tag{140a}$$

$$\mathbf{f}_G(s) = \mathbf{f}_{G,k}\delta(s - t_k)\Delta t \quad , \quad t_k \le s < t_{k+1} \tag{140b}$$

$$\mathbf{f}_M(s) = \mathbf{f}_{M,k}\delta(s - t_k)\Delta t \quad , \quad t_k \le s < t_{k+1} \tag{140c}$$

Substituting Eqs. 140a–140c into Eq. 139 and performing the integration gives

$$\mathbf{z}_{k+1} = \mathbf{e}^{\mathbf{A}\Delta t}\,\mathbf{z}_k + \Delta t\,\mathbf{e}^{\mathbf{A}\Delta t}\mathbf{H}\mathbf{a}_k + \Delta t\,\mathbf{e}^{\mathbf{A}\Delta t}\mathbf{B}\mathbf{f}_{G,k} + \Delta t\,\mathbf{e}^{\mathbf{A}\Delta t}\mathbf{B}\mathbf{f}_{M,k} \tag{141}$$

where $\mathbf{z}_k$, $\mathbf{a}_k$, $\mathbf{f}_{G,k}$, and $\mathbf{f}_{M,k}$ are the discretized forms of $\mathbf{z}(t)$, $\mathbf{a}(t)$, $\mathbf{f}_G(t)$, and $\mathbf{f}_M(t)$, respectively. Let

$$\mathbf{F}_d = \mathbf{e}^{\mathbf{A}\Delta t}, \quad \mathbf{H}_d = \mathbf{e}^{\mathbf{A}\Delta t}\mathbf{H}\Delta t, \quad \mathbf{B}_d = \mathbf{e}^{\mathbf{A}\Delta t}\mathbf{B}\Delta t \tag{142}$$

Then Eq. 141 becomes

$$\mathbf{z}_{k+1} = \mathbf{F}_d\mathbf{z}_k + \mathbf{H}_d\mathbf{a}_k + \mathbf{B}_d\mathbf{f}_{G,k} + \mathbf{B}_d\mathbf{f}_{M,k} \tag{143}$$

In Eq. 143, both equivalent force terms $\mathbf{f}_{G,k}$ and $\mathbf{f}_{M,k}$ are functions of the column axial forces at time step k. Therefore, Eq. 143 represents the recursive equation for calculating the dynamic response of moment-resisting framed structures while considering updates on geometric nonlinearity as the axial compressive force in columns changes with time.

For the case where updates on geometric nonlinearity are ignored in the nonlinear dynamic analysis, the $\overline{\mathbf{K}}_G(t)$ matrix as given in Eq. 128 becomes $\overline{\mathbf{K}}_G(t) = \mathbf{0}$. Therefore, from the same equation, $\overline{\mathbf{K}}(t) = \overline{\mathbf{K}}_L$. Then it follows from Eq. 136b that

$$\mathbf{f}_G(t) = [\mathbf{0}] \cdot \mathbf{x}_d(t) = \mathbf{0} \tag{144a}$$

$$\mathbf{f}_M(t) = \overline{\mathbf{K}}(t)\mathbf{x}''_d(t) = \overline{\mathbf{K}}_L\mathbf{x}''_d(t) \tag{144b}$$

and Eq. 143 becomes

$$\mathbf{z}_{k+1} = \mathbf{F}_d\mathbf{z}_k + \mathbf{H}_d\mathbf{a}_k + \mathbf{G}_d\mathbf{x}''_{d,k} \tag{145}$$

where

$$\mathbf{G}_d = \mathbf{B}_d\overline{\mathbf{K}}_o = \mathbf{e}^{\mathbf{A}\Delta t}\begin{bmatrix}\mathbf{0}\\ \mathbf{m}_{dd}^{-1}\end{bmatrix}\overline{\mathbf{K}}_o\Delta t = \mathbf{e}^{\mathbf{A}\Delta t}\begin{bmatrix}\mathbf{0}\\ \mathbf{m}_{dd}^{-1}\overline{\mathbf{K}}_L\end{bmatrix}\Delta t \tag{146}$$

and $\mathbf{x}''_{d,k}$ representing the discretized forms of $\mathbf{x}''_d(t)$. Equation 145 represents the recursive equation for calculating the nonlinear dynamic response of moment-resisting framed structures without updates on geometric nonlinearity as the axial compressive force in columns changes with time.

To perform nonlinear dynamic analysis, either Eq. 143 or Eq. 145 is used in conjunction with Eqs. 126b and 126c, rewritten here in discretized forms:

$$\mathbf{M}_{k+1} + \overline{\mathbf{K}}''_{k+1}\Delta\boldsymbol{\Theta}'' = \overline{\mathbf{K}}'^{T}_{k+1}\mathbf{x}_{d,k+1} - \overline{\mathbf{K}}''_{k+1}\boldsymbol{\Theta}''_k \tag{147}$$

$$\mathbf{x}''_{d,k+1} = \overline{\mathbf{K}}^{-1}_{k+1}\overline{\mathbf{K}}'_{k+1}\boldsymbol{\Theta}''_{k+1} \tag{148}$$

where $\mathbf{x}_{d,k}$, $\boldsymbol{\Theta}''_k$, and $\mathbf{M}_k$ are the discretized forms of $\mathbf{x}_d(t)$, $\boldsymbol{\Theta}''(t)$, and $\mathbf{M}(t)$, respectively, $\Delta\boldsymbol{\Theta}'' = \boldsymbol{\Theta}''_{k+1} - \boldsymbol{\Theta}''_k$, and $\overline{\mathbf{K}}_k$, $\overline{\mathbf{K}}'_k$, and $\overline{\mathbf{K}}''_k$ are the stiffness matrices at

Layout: T1 Standard | Book ID: 330342_1_En | Book ISBN: 978-3-319-47796-1
Chapter No.: 6 | Date: 30-9-2016 Time: 7:37 pm | Page: 41/47

time step k computed using the axial forces in columns at the same time step. Note that the stiffness matrices in Eqs. 147 and 148 are written in terms of time step $k+1$. However, the axial forces in columns at time step $k+1$ are unknown prior to the calculation of moments and change in plastic rotations, which means Eq. 147 requires an iterative procedure in the solution and may be difficult to execute. Therefore, the stiffness matrices in these two equations are approximated by replacing with those at time step k, i.e.,

$$\mathbf{M}_{k+1} + \overline{\mathbf{K}}''_k \Delta\boldsymbol{\Theta}'' = \overline{\mathbf{K}}'^T_k \mathbf{x}_{k+1} - \overline{\mathbf{K}}'_k \boldsymbol{\Theta}''_k \tag{149}$$

$$\mathbf{x}''_{k+1} = \overline{\mathbf{K}}_k^{-1} \overline{\mathbf{K}}'_k \boldsymbol{\Theta}''_{k+1} \tag{150}$$

If updates to geometric nonlinearity are ignored throughout the time history analysis, further approximation can be performed (as demonstrated in the comparison of responses in Sects. 4.4 and 4.5) by simplifying the stiffness matrices as:

$$\overline{\mathbf{K}}_k = \overline{\mathbf{K}}(0) = \overline{\mathbf{K}}_L, \quad \overline{\mathbf{K}}'_k = \overline{\mathbf{K}}'(0) = \overline{\mathbf{K}}'_L, \quad \overline{\mathbf{K}}''_k = \overline{\mathbf{K}}''(0) = \overline{\mathbf{K}}''_L \tag{151}$$

where $\overline{\mathbf{K}}'_L$ and $\overline{\mathbf{K}}''_L$ (and $\overline{\mathbf{K}}_L$ as previously defined in Eq. 131) are the linearized condensed stiffness matrices with geometric nonlinearity derived from the gravity load on the frame only. Then Eqs. 149 and 150 become

$$\mathbf{M}_{k+1} + \overline{\mathbf{K}}''_L \Delta\boldsymbol{\Theta}'' = \overline{\mathbf{K}}'^T_L \mathbf{x}_{d,k+1} - \overline{\mathbf{K}}''_L \boldsymbol{\Theta}''_k \tag{152}$$

$$\mathbf{x}''_{d,k+1} = \overline{\mathbf{K}}_L^{-1} \overline{\mathbf{K}}'_L \boldsymbol{\Theta}''_{k+1} \tag{153}$$

Equations 145, 152, and 153 represent the set of equations for solving the nonlinear dynamic analysis problems when no update to geometric nonlinearity due to changes in axial force is performed.

Finally, the absolute acceleration vector (i.e., $\ddot{\mathbf{y}}_d(t) = \ddot{\mathbf{x}}_d(t) + \ddot{\mathbf{g}}_d(t)$) can be computed by rewriting Eq. 126a in discretized form as

$$\ddot{\mathbf{y}}_{d,k} = -\mathbf{m}_{dd}^{-1}\mathbf{c}_{dd}\dot{\mathbf{x}}_{d,k} - \mathbf{m}_{dd}^{-1}\overline{\mathbf{K}}_k\left(\mathbf{x}_{d,k} - \mathbf{x}''_{d,k}\right) - \mathbf{m}_{dd}^{-1}\mathbf{K}_a\mathbf{x}_{d,k} \tag{154}$$

where $\dot{\mathbf{x}}_{d,k}$ and $\ddot{\mathbf{y}}_{d,k}$ are the discretized forms of $\dot{\mathbf{x}}_d(t)$ and $\ddot{\mathbf{y}}_d(t)$, respectively.

5.3 *Implementation of the Dynamic Analysis Procedure to the One-Story Frame*

As an example of the above derivation, consider the same configuration of a one-story one-bay moment-resisting frame as shown in Fig. 6 but with different

Layout: T1 Standard | Book ID: 330342_1_En | Book ISBN: 978-3-319-47796-1
Chapter No.: 6 | Date: 30-9-2016 Time: 7:37 pm | Page: 42/47

member properties. First, let the members be axially rigid. This gives a total of 3 DOFs (i.e., $n = 3$) and 6 PHLs (i.e., $m = 6$) as shown in the figure. The global stiffness matrices have been presented in Eqs. 56a–56c.

Assume that the frame has a mass of $m_{dd} = 318.7$ Mg and a damping of 0 % (i.e., $c_{dd} = 0.0$) at DOF #1, while the mass moment of inertia at DOFs #2 and #3 are ignored. This gives $d = 1$ and $r = 2$. Note that $d + r = n$. Therefore, static condensation can be applied to eliminate the DOFs for x_2 and x_3. For the beam and columns, let $E = 200$ GPa, $I_b = I_c = 4.995 \times 10^8$ mm^4, $L_b = 7.62$ m, and $L_c = 4.57$ m. Assume that the plastic hinges exhibit elastic-plastic behavior with plastic moment capacities of $M_b = 3130$ kN-m for the beam and $M_c = 3909$ kN-m for the two columns. Also, let the gravity load be $P = 5338$ kN. Assuming no update of geometric nonlinearity due to changes in axial forces in columns is performed, the condensed stiffness matrices $\overline{\mathbf{K}}_L$, $\overline{\mathbf{K}}'_L$, and $\overline{\mathbf{K}}''_L$ based on Eq. 117 become:

$$\overline{K}_L = \overline{K}_e = 10018\,\text{kN/m} \tag{155a}$$

$$\overline{\mathbf{K}}'_L = [\,16907 \quad 11331 \quad 16907 \quad 11331 \quad -11331 \quad -11331\,]\,\text{kN} \tag{155b}$$

$$\overline{\mathbf{K}}''_L = \begin{bmatrix} 56761 & 13494 & 2458 & 4585 & -13494 & -4585 \\ 13494 & 25173 & 4585 & 8554 & -25173 & -8554 \\ 2458 & 4585 & 56761 & 13494 & -4585 & -13494 \\ 4585 & 8554 & 13494 & 25173 & -8554 & -25173 \\ -13494 & -25173 & -4585 & -8554 & 25173 & 8554 \\ -4585 & -8554 & -13494 & -25173 & 8554 & 25173 \end{bmatrix} \text{kN} - \text{m/rad} \tag{155c}$$

The period of vibration T is calculated as:

$$T = 2\pi\sqrt{m_{dd}/\overline{K}_L} = 2\pi\sqrt{318.7/10017} = 1.121\,\text{s} \tag{156}$$

With a time step size of $\Delta t = 0.01$ s and assuming no updates to the geometric nonlinearity is performed, the transition matrices are calculated as:

$$\mathbf{A} = \begin{bmatrix} 0 & 1 \\ -31.43 & 0 \end{bmatrix}, \quad \mathbf{H} = \begin{bmatrix} 0 \\ -1 \end{bmatrix}, \quad \mathbf{B} = \begin{bmatrix} 0 \\ 0.5495 \end{bmatrix} \tag{157a}$$

$$\mathbf{F}_d = \mathbf{e}^{\mathbf{A}\Delta t} = \begin{bmatrix} 0.998429 & 0.009995 \\ -0.31415 & 0.998429 \end{bmatrix}, \mathbf{H}_d = \begin{bmatrix} -0.00010 \\ -0.00998 \end{bmatrix}, \mathbf{G}_d = \begin{bmatrix} 0.00314 \\ 0.31381 \end{bmatrix} \tag{157b}$$

and Eqs. 145, 152, and 153 for performing the nonlinear dynamic analysis become

Layout: T1 Standard | Book ID: 330342_1_En | Book ISBN: 978-3-319-47796-1
Chapter No.: 6 | Date: 30-9-2016 | Time: 7:37 pm | Page: 43/47

$$\begin{Bmatrix} x_1 \\ \dot{x}_1 \end{Bmatrix}_{k+1} = \begin{bmatrix} 0.998429 & 0.009995 \\ -0.31415 & 0.998429 \end{bmatrix} \begin{Bmatrix} x_1 \\ \dot{x}_1 \end{Bmatrix}_k + \begin{bmatrix} -0.00010 \\ -0.00998 \end{bmatrix} a_k + \begin{bmatrix} 0.00314 \\ 0.31381 \end{bmatrix} x''_{d,k} \tag{158a}$$

$$\begin{Bmatrix} M_1 \\ M_2 \\ M_3 \\ M_4 \\ M_5 \\ M_6 \end{Bmatrix}_{k+1} + \begin{bmatrix} 56761 & 13494 & 2458 & 4585 & -13494 & -4585 \\ 13494 & 25173 & 4585 & 8554 & -25173 & -8554 \\ 2458 & 4585 & 56761 & 13494 & -4585 & -13494 \\ 4585 & 8554 & 13494 & 25173 & -8554 & -25173 \\ -13494 & -25173 & -4585 & -8554 & 25173 & 8554 \\ -4585 & -8554 & -13494 & -25173 & 8554 & 25173 \end{bmatrix} \begin{Bmatrix} \Delta\theta''_1 \\ \Delta\theta''_2 \\ \Delta\theta''_3 \\ \Delta\theta''_4 \\ \Delta\theta''_5 \\ \Delta\theta''_6 \end{Bmatrix}$$

$$= \begin{bmatrix} 16907 \\ 11329 \\ 16907 \\ 11329 \\ -11329 \\ -11329 \end{bmatrix} x_{1,k+1} - \begin{bmatrix} 56761 & 13494 & 2458 & 4585 & -13494 & -4585 \\ 13494 & 25173 & 4585 & 8554 & -25173 & -8554 \\ 2458 & 4585 & 56761 & 13494 & -4585 & -13494 \\ 4585 & 8554 & 13494 & 25173 & -8554 & -25173 \\ -13494 & -25173 & -4585 & -8554 & 25173 & 8554 \\ -4585 & -8554 & -13494 & -25173 & 8554 & 25173 \end{bmatrix} \begin{Bmatrix} \theta''_1 \\ \theta''_2 \\ \theta''_3 \\ \theta''_4 \\ \theta''_5 \\ \theta''_6 \end{Bmatrix}_k \tag{158b}$$

$$x''_{d,k+1} = \frac{1}{10017} \begin{bmatrix} 16907 & 11329 & 16907 & 11329 & -11329 & -11329 \end{bmatrix} \begin{Bmatrix} \theta''_1 \\ \theta''_2 \\ \theta''_3 \\ \theta''_4 \\ \theta''_5 \\ \theta''_6 \end{Bmatrix}_{k+1} \tag{158c}$$

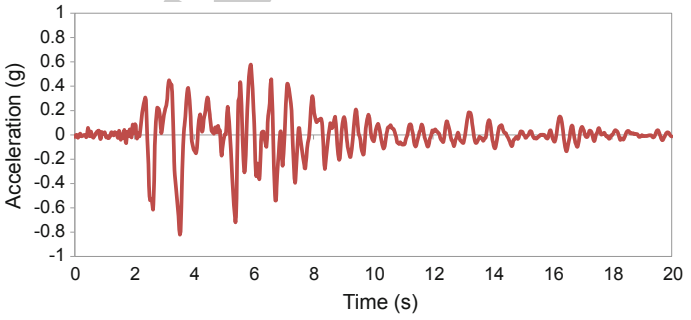

Fig. 8 1995 Kobe earthquake ground acceleration at Kajima station, component 000, with a peak ground acceleration of 0.821 g

Layout: T1 Standard | Book ID: 330342_1_En | Book ISBN: 978-3-319-47796-1
Chapter No.: 6 | Date: 30-9-2016 Time: 7:37 pm | Page: 44/47

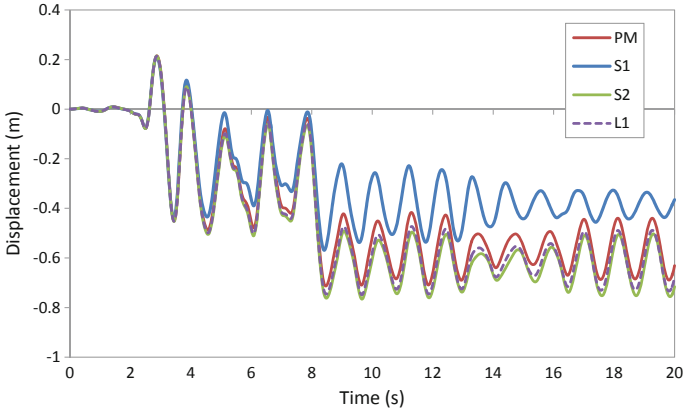

Fig. 9 Displacement response comparisons of the one-story frame using the proposed method (PM) with two small-displacement-based structural analysis software packages (S1 and S2) and a large-displacement-based finite element software package (L1)

Equation 158a–158c represents the set of recursive equations used for the entire nonlinear dynamic analysis. Note that the method for solving Eq. 158b is similar to those discussed in Sects. 4.4 and 4.5, where an iterative procedure is used to determine whether each plastic hinges is at the loading phase (i.e., plastic rotation becomes the unknown) or at the unloading phase (i.e., moment becomes the unknown).

The frame is now subjected to the 1995 Kobe earthquake ground motion as shown in Fig. 8 but magnified with a scale factor of 1.3 to produce larger displacement response and more yielding in the plastic hinges. The global displacement response at DOF #1 is plotted in Fig. 9 using the currently proposed method (PM) of nonlinear analysis. In addition, two small-displacement-based structural analysis software packages (here labeled as S1 that uses $P-\Delta$ stiffness as shown in Eq. 30 and S2 that uses geometric stiffness as shown in Eq. 29) and a large-displacement-based finite element analysis software package (here labeled as L1) are used to develop the same one-story one-bay moment-resisting frame model as shown in Fig. 6, and the undamped displacement responses obtained from S1 and S2 are also plotted in Fig. 9 for comparisons. Note that even though using 0 % damping is an idealized situation, it helps eliminate the potentially differing effects of using damping parameters on the responses that may occur due to differences in damping formulations used in various software packages.

As shown in Fig. 9, it is observed that the proposed method (PM) produces a "global" response that is comparable to other software packages that use different material nonlinearity and geometric nonlinearity formulations. At such a large displacement response of the frame, the large-displacement-based finite element analysis software package L1 is assumed to give accurate results; therefore, it serves as a benchmark for other small-displacement-based software packages. It is

Layout: T1 Standard | Book ID: 330342_1_En | Book ISBN: 978-3-319-47796-1
Chapter No.: 6 | Date: 30-9-2016 Time: 7:37 pm | Page: 45/47

observed that while S1 differs noticeably from the L1 prediction, S2 performs slightly better than the PM in the displacement response.

Figure 10 shows the plastic hinge moment responses at PHLs #1, #3, #5, and #6 of the one-story one-bay frame among the same software packages used in the study. As shown in this figure, the L1 results show that the moment responses at all the plastic hinges should be skewed to the positive direction. However, only the proposed method (PM) captures this behavior, while S1 captures this behavior to a lesser extent and S2 misses the behavior completely. This suggests that starting from the basic principles at the element level is important in capturing the local responses of the structure.

Finally, Fig. 11 shows the plastic rotations responses at PHLs #1, #3, #5, and #6 of the one-story one-bay frame using the small-displacement-based structural analysis software packages. The large-displacement-based finite element software package L1 produces plastic strain as the output, yet the conversion from plastic strain to plastic rotation is not readily available. Therefore, the output from L1 is not plotted in the figure. By comparing the proposed method (PM) with S1 in Fig. 11, it can be seen that even though the local plastic rotation responses change suddenly (jumps) due to yielding at the same time steps, the magnitudes of the changes are different. Given the performance accuracy of PM in Fig. 10, this suggests that the software package S1 may not have addressed the effect of plastic rotation on the residual response of the structure appropriately. Finally, at such a large displacement response as shown in Fig. 9, software package S2 predicts only a slight

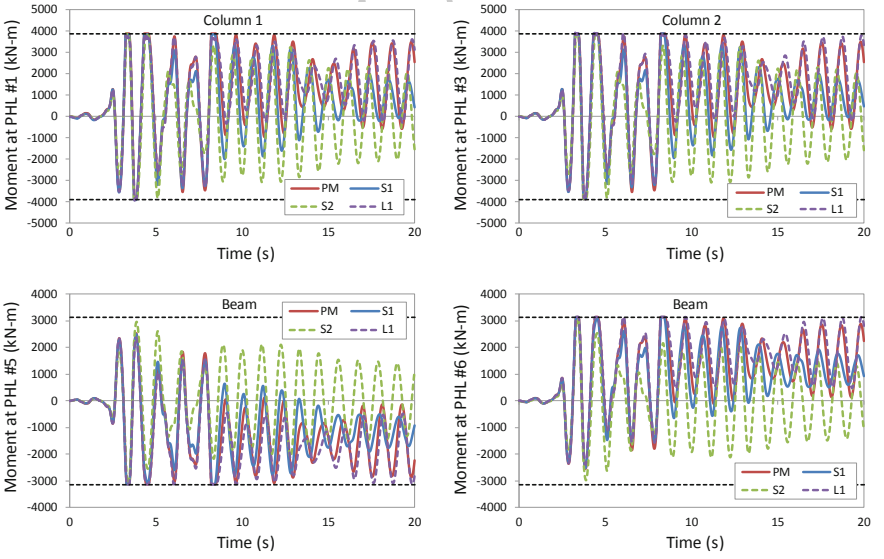

Fig. 10 Moment response comparisons at various plastic hinge locations using the proposed method (PM) with two small-displacement-based structural analysis software packages (S1 and S2) and a large-displacement-based finite element software package (L1)

Layout: T1 Standard | Book ID: 330342_1_En | Book ISBN: 978-3-319-47796-1
Chapter No.: 6 | Date: 30-9-2016 | Time: 7:37 pm | Page: 46/47

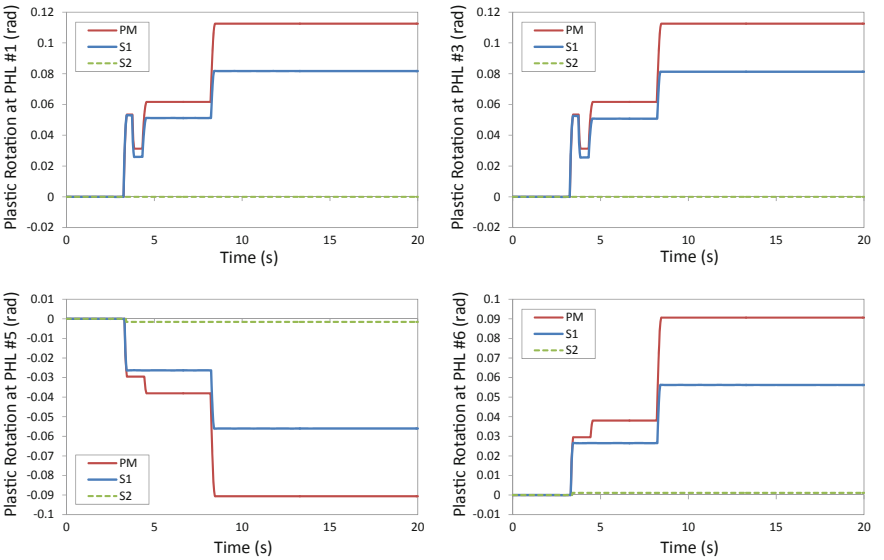

Fig. 11 Plastic rotation response comparisons at various plastic hinge locations using the proposed method (PM) with two small-displacement-based structural analysis software packages (S1 and S2) and a large-displacement-based finite element software package (L1)

damage in the plastic rotation responses shown in Fig. 11 with fairly elastic moment responses in Fig. 10 throughout the analysis. This suggests that there may be a fundamental issue in calculating the local response that software package S1 may have missed.

6 Conclusion

Plastic rotation in moment-resisting frame is an important parameter in the assessment process for performance-based seismic engineering, and therefore it needs to be calculated correctly. In this research, basic principles were used to derive the stiffness matrices of a column member with axial load to capture the interaction between geometric nonlinearity and material nonlinearity. This results in a method for capturing the plastic rotation demand for both nonlinear static analysis and nonlinear dynamic analysis that produces displacement results comparable with the large-displacement-based finite element software package L1 used in the study. It also suggests that this method is an improvement to the two small-displacement-based software packages S1 and S2 used in the study. While there are many structural analysis software packages available that consider both geometric and material nonlinearities, it is unclear which ones have addressed the interaction appropriately. Therefore, engineers should be careful in assessing plastic

Layout: T1 Standard | Book ID: 330342_1_En | Book ISBN: 978-3-319-47796-1
Chapter No.: 6 | Date: 30-9-2016 Time: 7:37 pm | Page: 47/47

rotation responses in moment-resisting frames with large displacement, where significant material nonlinearity is coupled with significant geometric nonlinearity. This leads to a bigger question as to the accuracy and reliability on assessing damages in moment-resisting framed structures based on the ASCE/SEI 41-13 recommendations, which is something that eventually must be addressed in the future updates of the standard.

The method for calculating plastic rotations developed in this research was based on two-dimensional analysis. Two-dimensional stiffness matrices for beams seem appropriate, but these matrices may need to be extended to three-dimensions for columns when biaxial bending is significant. In addition, elastic-plastic behavior was used in the examples for simplicity of illustrations on the calculation method. However, in order to capture the actual behavior more accurately, a hysteretic bilinear model with post-capping degrading strength may be necessary. Therefore, further research in these areas are needed.

References

1. ASCE/SEI 41-13 (2013) Seismic evaluation and retrofit of existing buildings. American Society of Civil Engineers, Reston, VA
2. Domizio M, Ambrosini D, Curadelli O (2015) Experimental and numerical analysis to collapse of a framed structure subjected to seismic loading. Eng Struct 82:22–32
3. Eads L, Miranda E, Krawinkler H, Lignos DG (2013) An efficient method for estimating the collapse risk of structures in seismic regions. Earthquake Eng Struct Dyn 42(1):25–41
4. Grigorian M, Grigorian CE (2012) Lateral displacements of moment frames at incipient collapse. Eng Struct 44:174–185
5. Lignos DG, Krawinkler H, Whittaker AS (2011) Prediction and validation of sidesway collapse of two scale models of a 4-story steel moment frame. Earthquake Eng Struct Dyn 40 (7):807–825
6. Zareian F, Krawinkler H (2007) Assessment of probability of collapse and design for collapse safety. Earthquake Eng Struct Dyn 36(13):1901–1914
7. Bazant ZP, Cedolin L (2003) Stability of structures. Dover Publication, New York
8. Horne MZ, Merchant W (1965) The stability of frames. Pergamon Press, New York
9. Timoshenko SP, Gere JM (1961) Theory of elastic stability, 2nd edn. McGraw Hill, New York
10. Powell GH (2010) Modeling for structural analysis: behavior and basics. Computers and Structures Inc., California
11. McGuire W, Gallagher RH, Ziemian RD (2000) Matrix structural analysis. John Wiley and Sons, New York
12. Park JW, Kim SE (2008) Nonlinear inelastic analysis of steel-concrete composite beam-columns using the stability functions. Struct Eng Mech 30(6):763–785
13. Hibbeler RC (2012) Structural analysis, 8th edn. Prentice Hall, New Jersey, USA
14. Leet KM, Uang CM, Gilbert AM (2010) Fundamentals of structural analysis, 4th edn. McGraw Hill, New York, USA
15. Wilson EL (2010) Static and dynamic analysis of structures. Computers and Structures Inc., California